Chandra's 10 Year Legacy: Studies of Planets and Comets in the X-ray

***C.M. Lisse** (JHU APL); **A. Bhardwaj** (SPL); **K. Dennerl** (MPE); **S.J. Wolk** (CXC); **D. J. Christian** (CalState Northridge); **D. Bodewits** (NASA/GSFC); **M. Combi, T.H. Zurbuchen** (U. Mich); M. Dryer (NOAO)*

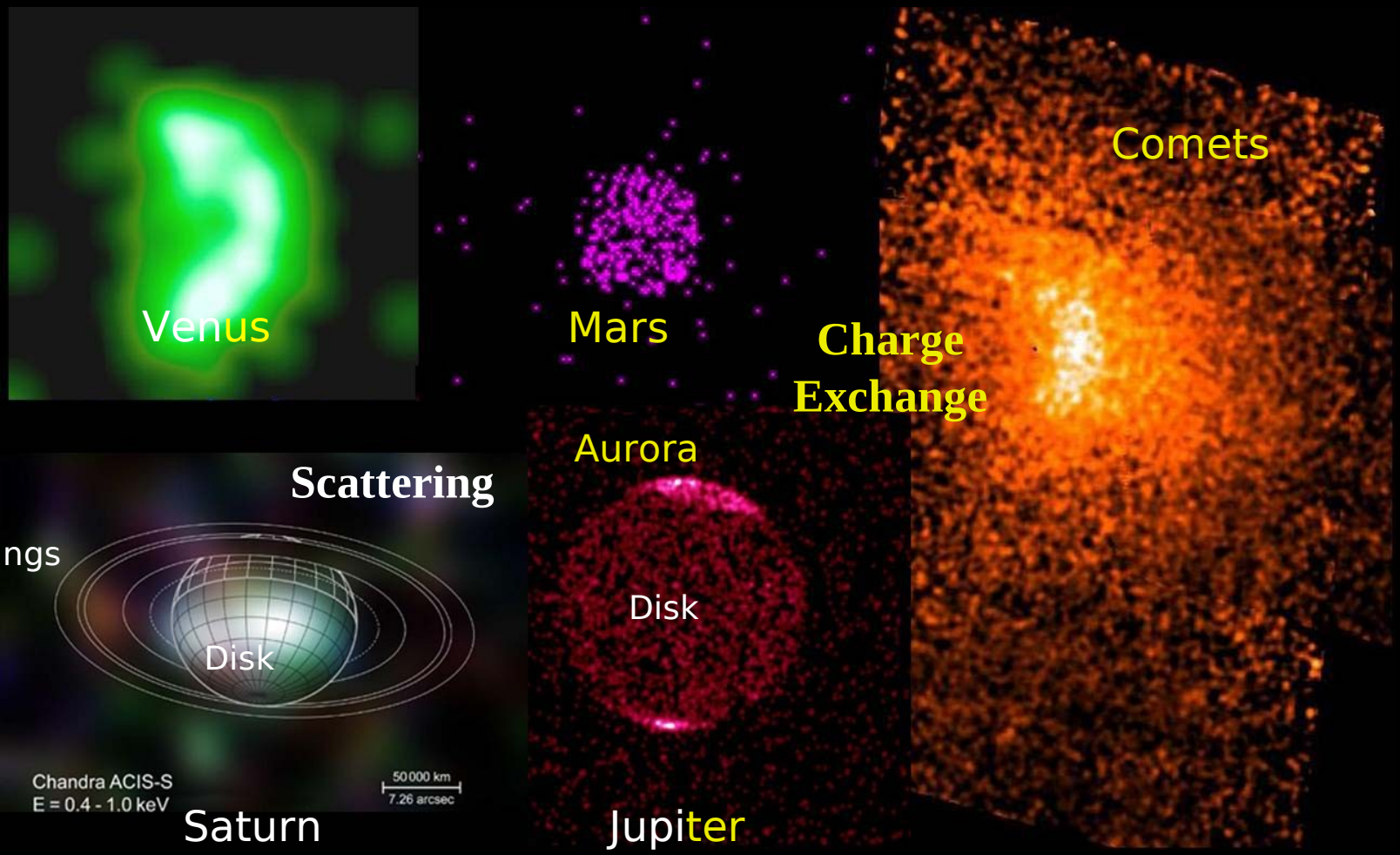

Some of the currently known sources of X-rays in the Solar System. The complete list incl's the Sun, Planets, Comets, Moons, the Io Flux Torus, and the Heliosphere itself. [See excellent review by Bhardwaj, Lisse, et al. 2007 and ESS 2008]

It all starts with the Sun, an average G2V MS star of 4.56 Gyr which actively emits L_x ~10^{27} erg/sec…

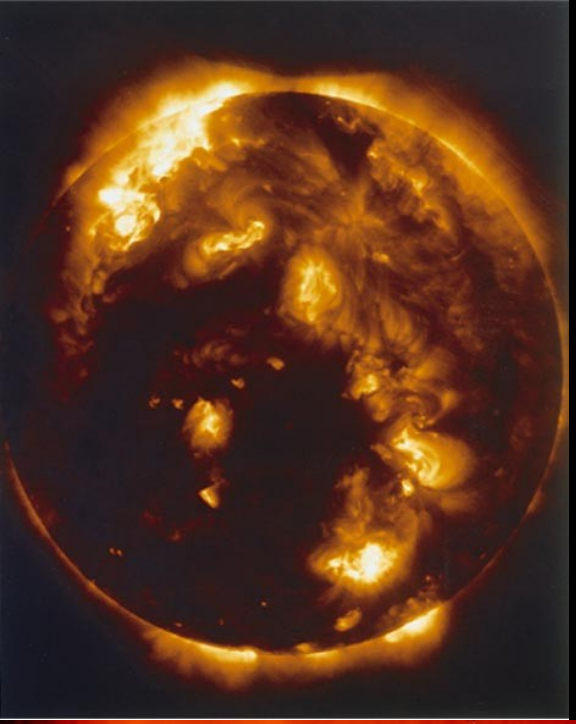

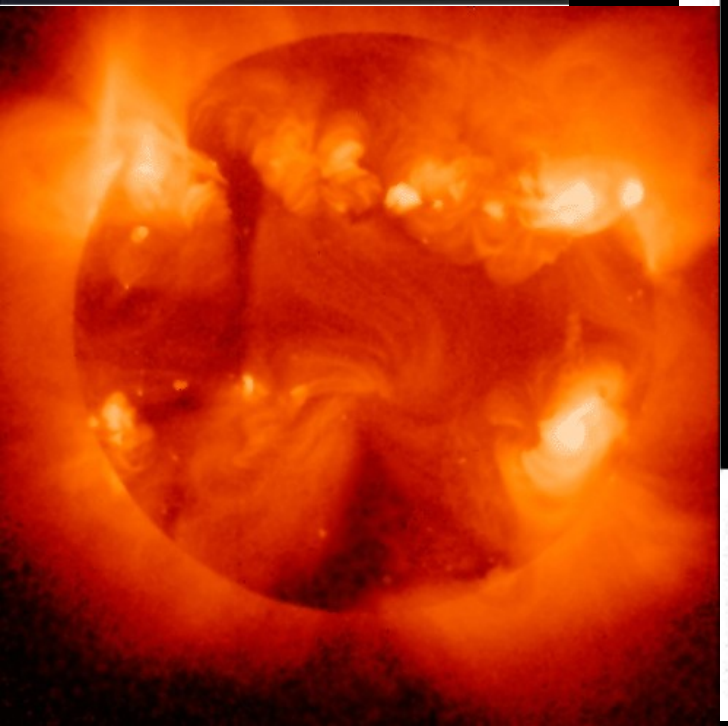

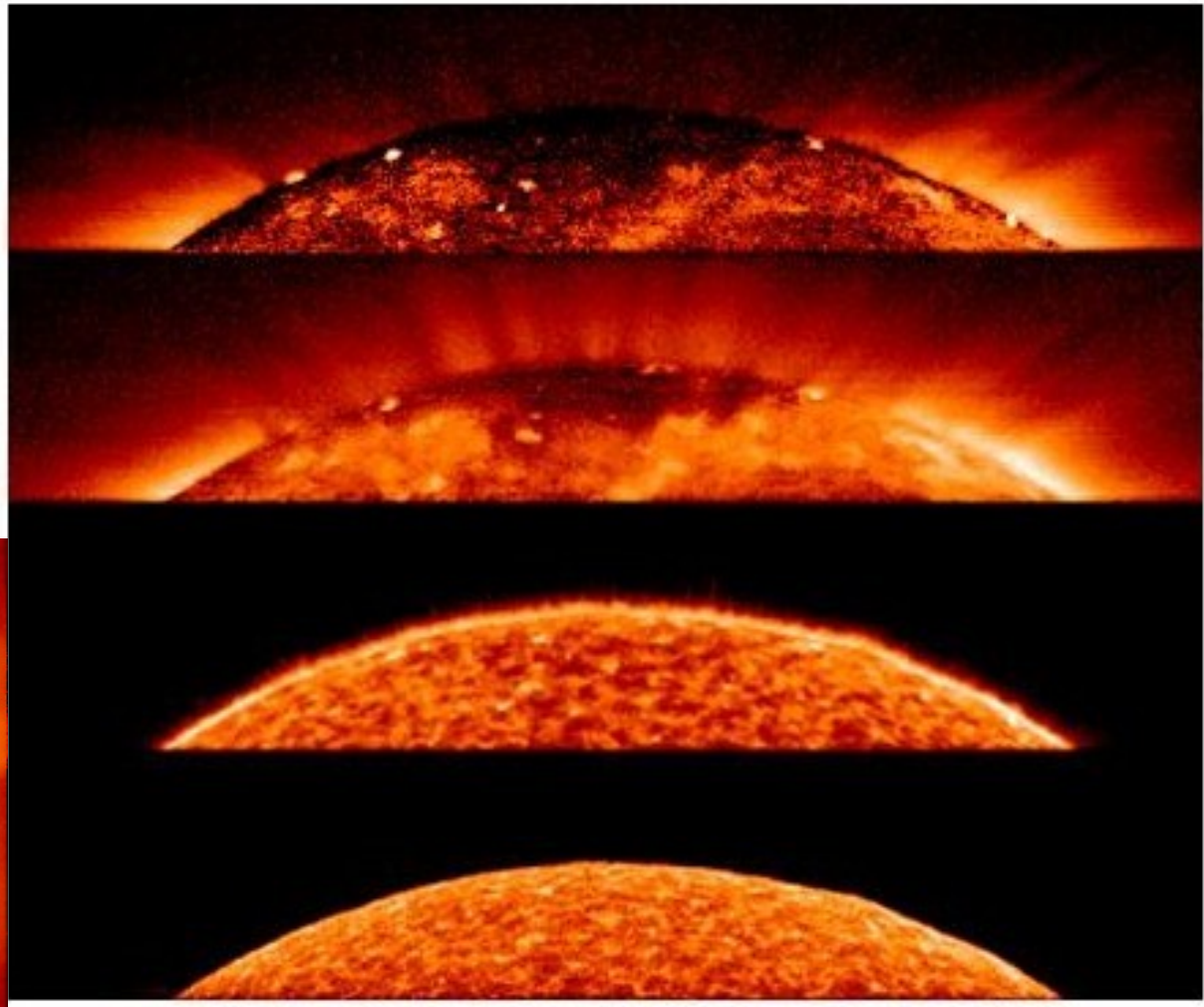

Anatomy of a coronal hole - Radiance maps in different emission lines (top to bottom):
The Fe XII (1241.990 Å) exposure outlines the coronal hole boundaries.
The Mg X (624.965 Å) image highlights the polar plumes and coronal bright points.
Spicules and a pronounced limb brightening can be seen in N V (1238.821 Å).
The C I (1249.405 Å) image shows the chromospheric network (ESA SP-1274, 2003).

…and Streams of Solar Wind p+, He^{+2}, & Highly Stripped Minor Ions (@ the ~10^{-3} abundance level) at M_{sw} ~ 10^{-14} $M_{\odot}$/yr into the heliosphere & interplanetary space.

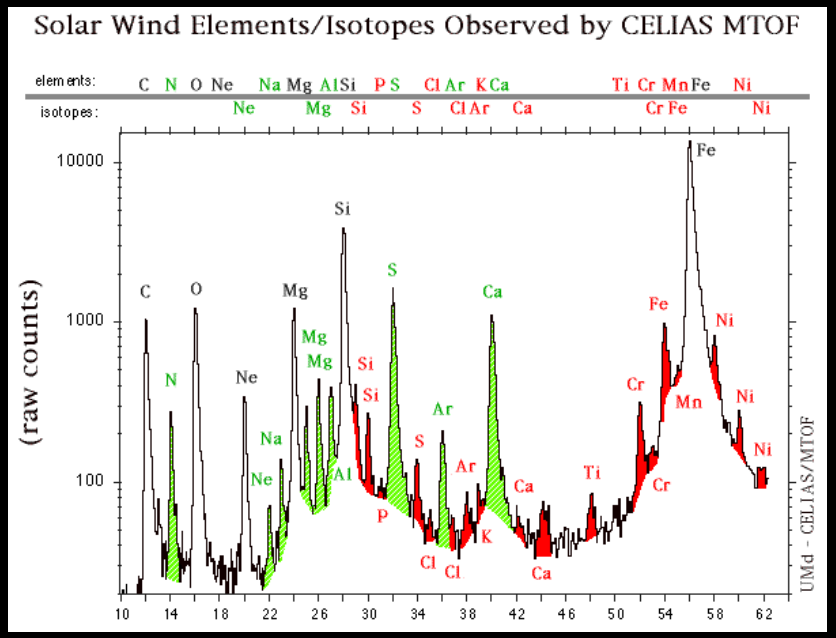

Ulysses : Solar wind properties near

solar minimum

solar maximum

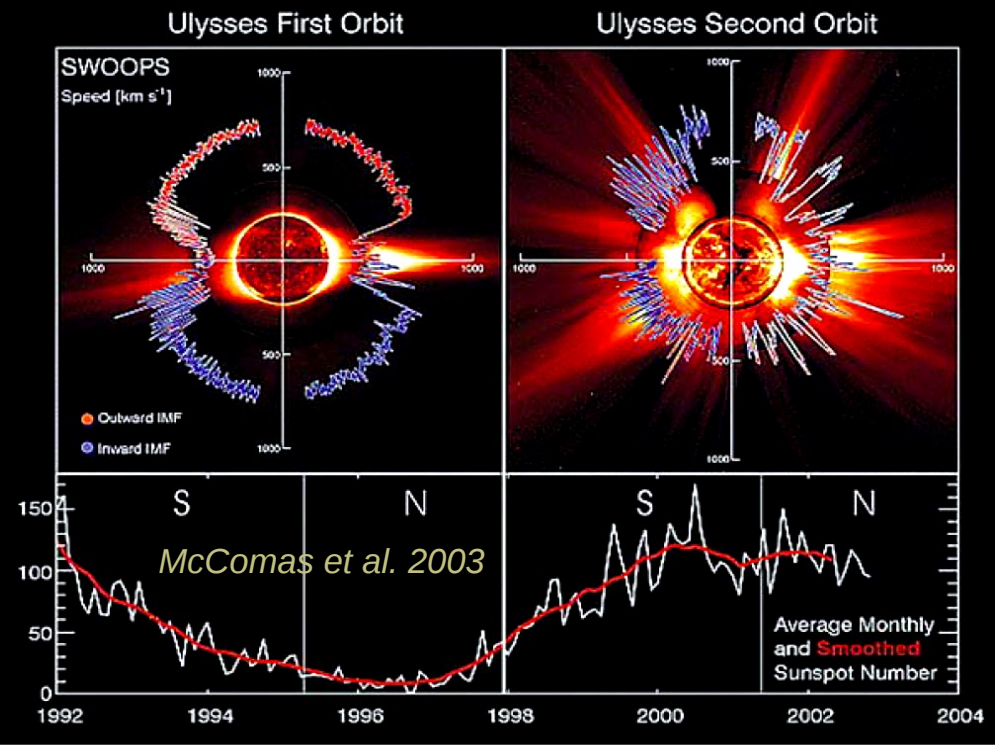

Polar Solar Wind:

fast (~700 km/s), low density, cold, less ionized, regular

Equatorial Solar Wind:

- Slow (~400 km/s), warm, more ionized, high density, quiet
- From coronal holes : fast, cold, less ionized, disturbed (like polar wind)
- With CMEs or flares : fast, hot, highly ionized, disturbed.

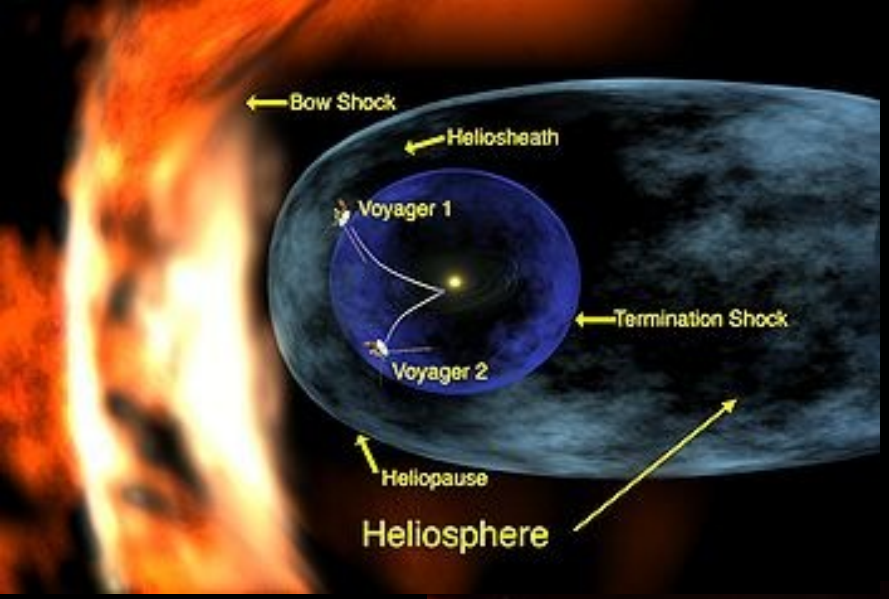

Our Solar System is awash in MK Solar Wind particles and High Energy photons from the Sun, driving soft (0.1 – 1.0 keV) X-ray emission in response from the interplanetary and heliospheric environments.

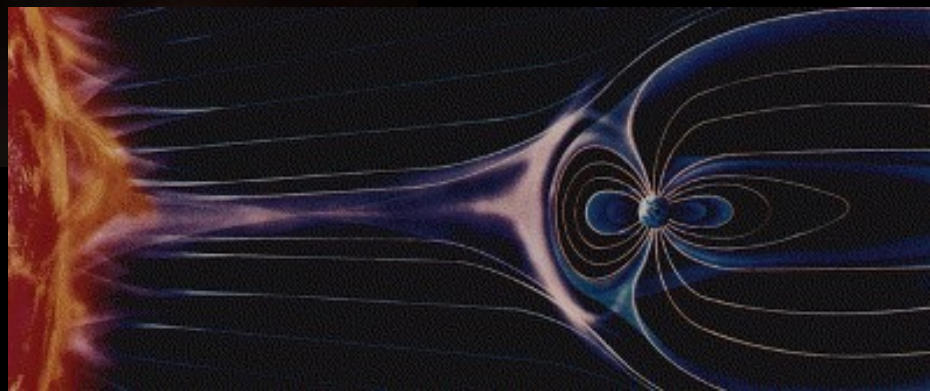

Example: Interaction between the Gravitationally Unbound Neutral Atmospheres of Comets and the Solar Wind

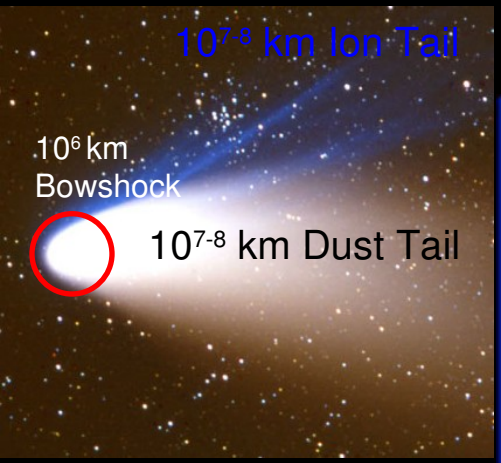

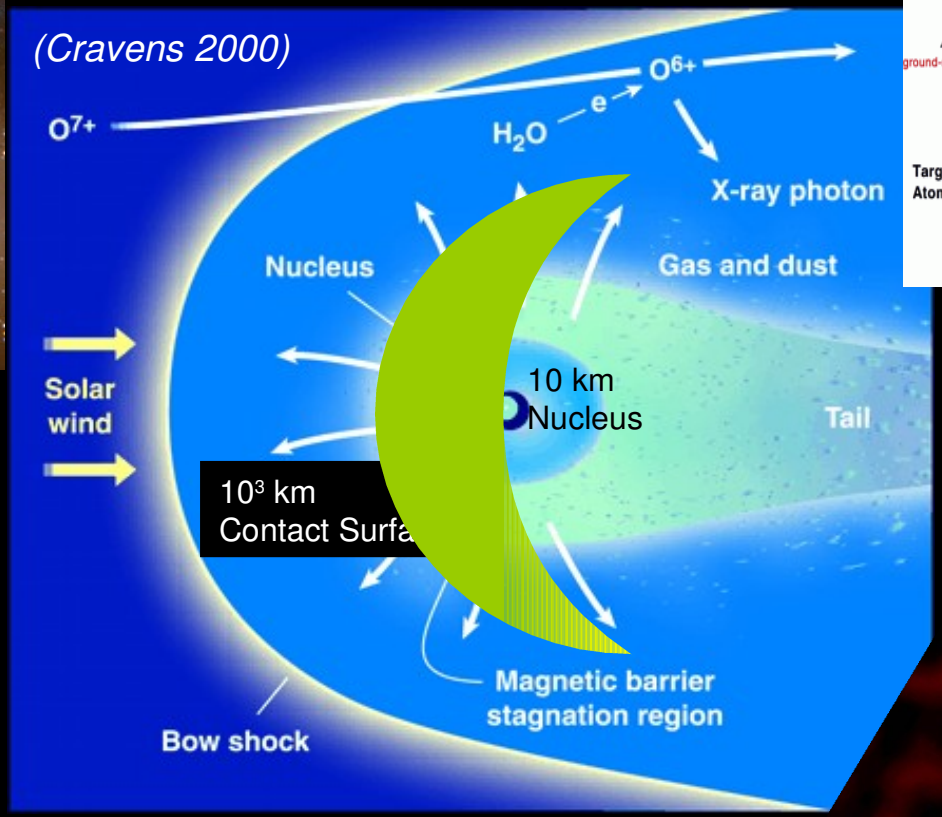

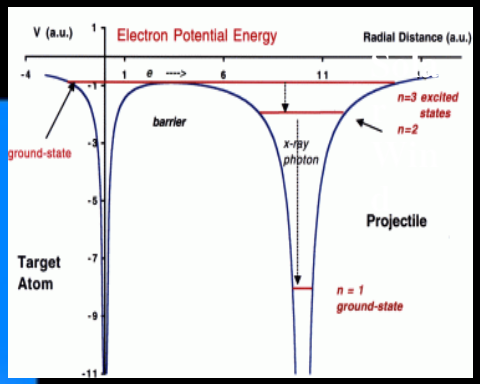

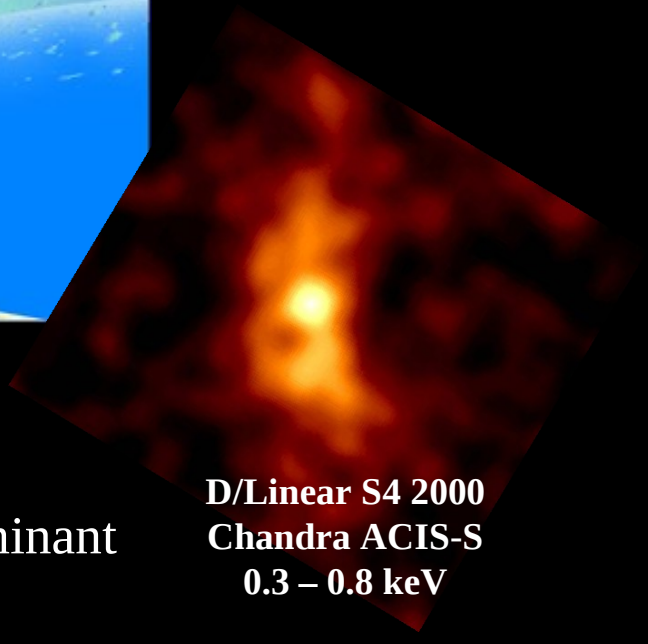

D/Linear S4 2000
Chandra ACIS-S
0.3 – 0.8 keV

Solar Wind Charge Exchange (SWCXE) is the Dominant Ionization Process for Outflowing Cometary Gases

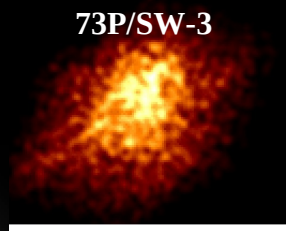

8P/Tuttle 2008 & 17P/Holmes 2007
Christian *et al.* 2009 (submitted)

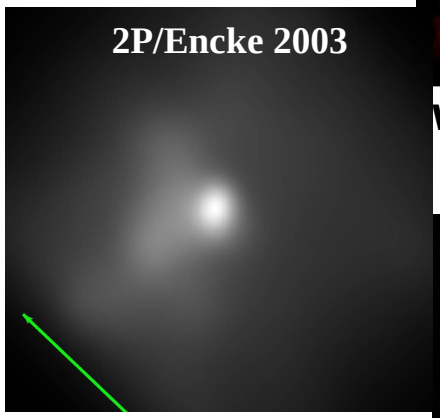

Wolk *et al.* 2009

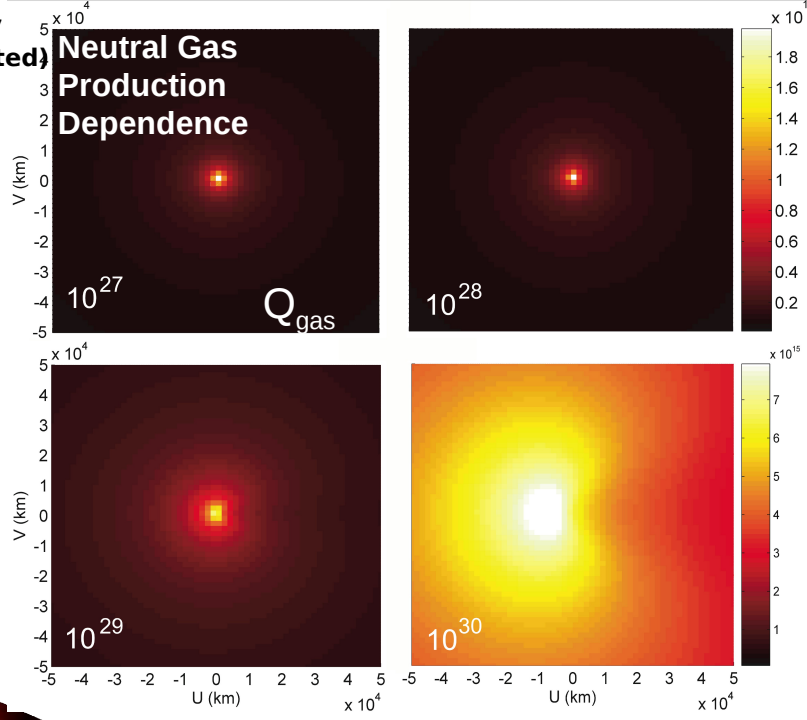

Lisse *et al.* 2005

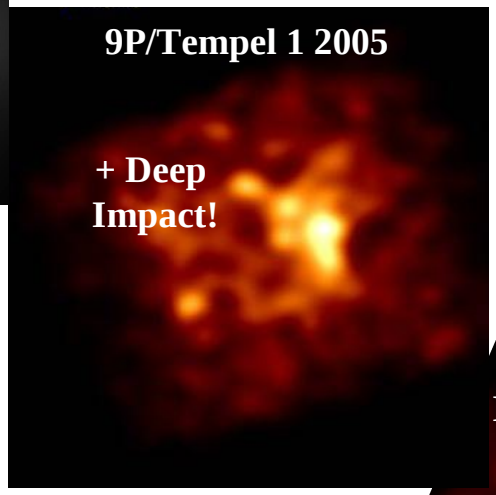

Lisse *et al.* 2007

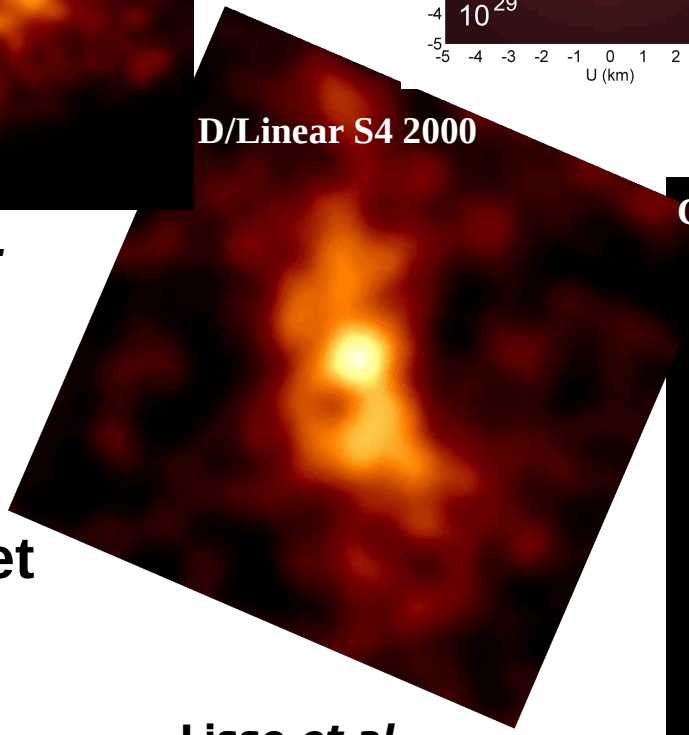

Lisse *et al.* 2001

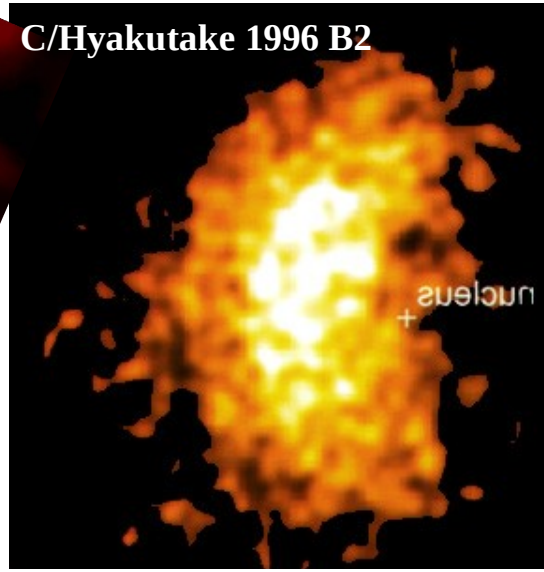

Lisse *et al* 1996

~10 Yrs of Solar Wind – Comet Neutral CXE Comet Morphologies : Sunward Facing, Coma Localized, Collisionally Thin or Thick

Comets observed with Chandra, 2000 – May 2008

17P/2007 (Holmes)??

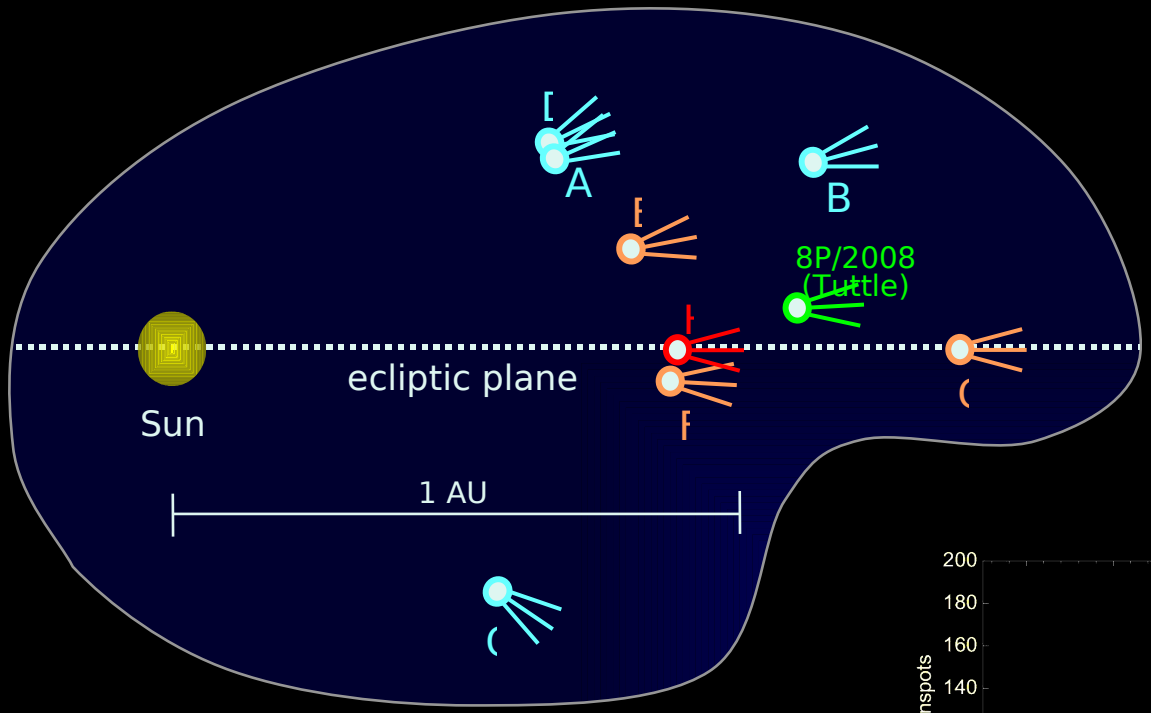

A: C/1999 S4 (LINEAR)

B: C/1999 T1 (McNaught-Hartley)

C: C/2000 WM1 (LINEAR)

D: 153P/2002 (Ikeya-Zhang)

E: 2P/2003 (Encke)

F: C/2001 Q4 (NEAT)

G: 9P/2005 (Tempel 1)

H: 73P/2006 (SW3-B)

I: 8P/2008 (Tuttle)

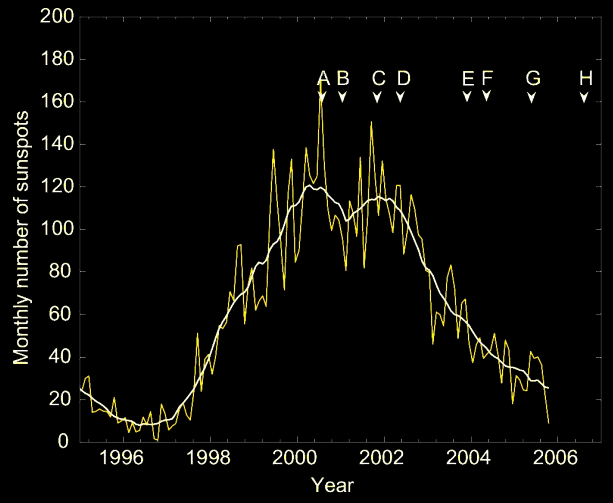

I:

Chandra spectra of comets:

Three competing emission features:

- C and N emission below 500 eV
- O VII emission at 565 eV
- O VIII emission at 654 eV

Bodewits et al. 2007

→ flux ratios of all observed comets:

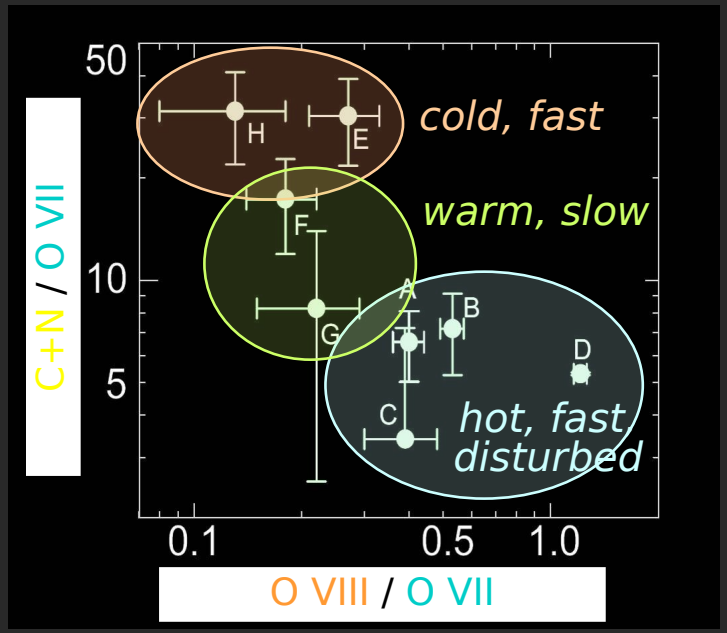

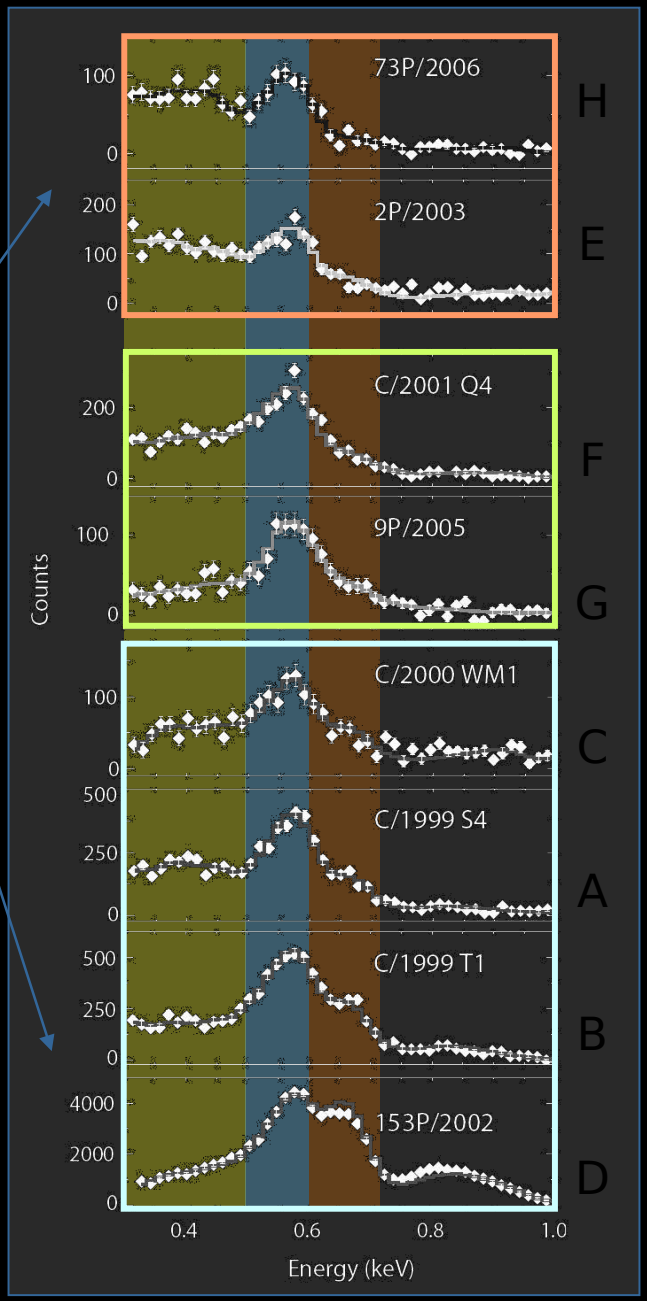

X-rays at the Earth : Auroral Precipitation + Atmospheric Scattering of Solar X-ray Radiation

Chandra : Soft e- Auroral X-rays

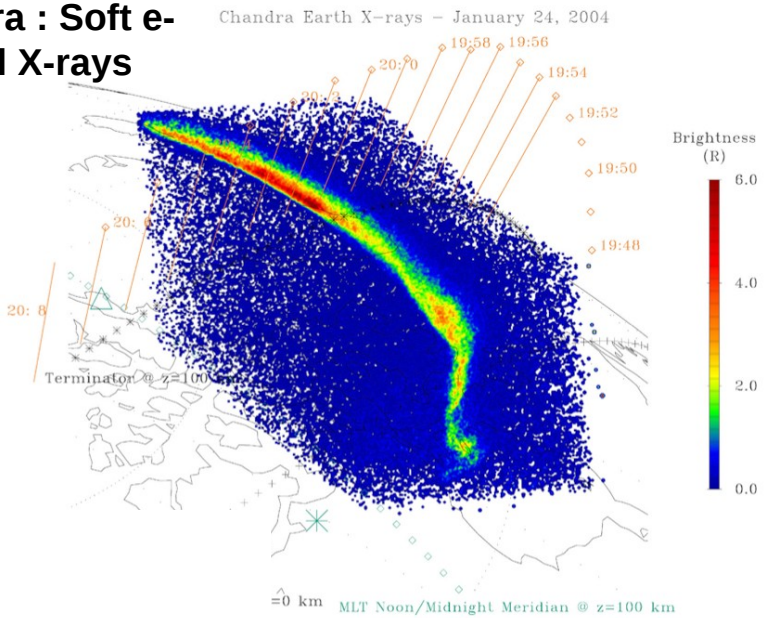

1 on January 24, 2004 showing a bright arc. The orbital location of satellite DMSP F13 is shown by s extending down to an altitude of 100 km (from Bhardwaj et al., 2007).

Polar PIXIE : 3-10 keV
SW Particle Auroral X-rays

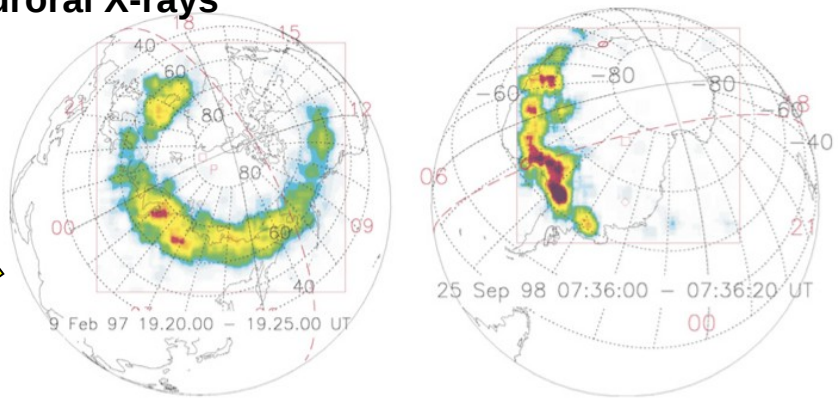

Fig. 5. Auroral X-ray images of the Earth from the Polar PIXIE instrument. To the left: 5 min accumulation of X-rays in the en from the northern hemisphere on February 9, 1997. To the right: 20 s accumulation of X-rays in the energy range 2.7–9.6 keV on S the southern hemisphere. 00, 06, 12 and 18 denote the magnetic local times.

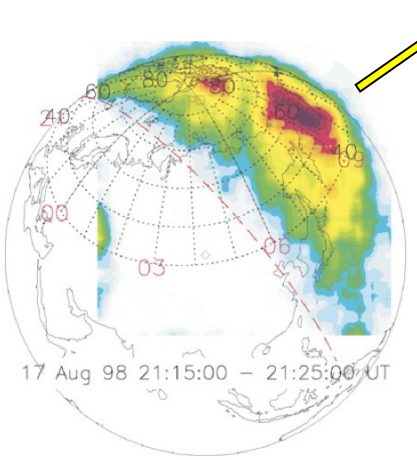

Fig. 8. X-ray image of Earth from the Polar PIXIE instrument for energy range 2.9–10.1 keV obtained on August 17, 1998, showing the dayside X-rays during a solar X-ray flare. The grid in the picture is in corrected geomagnetic coordinates, and the numbers shown in red are magnetic local time. The terminator at the surface of the Earth is shown as a red dashed line.

Polar PIXIE : 3-10 keV
In-Flare Scattering + Ar fluorescence

Lunar X-rays : Scattering on Day Side + SWCXE in Fore-Column on the Nightside

Dayside : O, Si, Mg, Al fluorescence lines from lunar soil + rock.

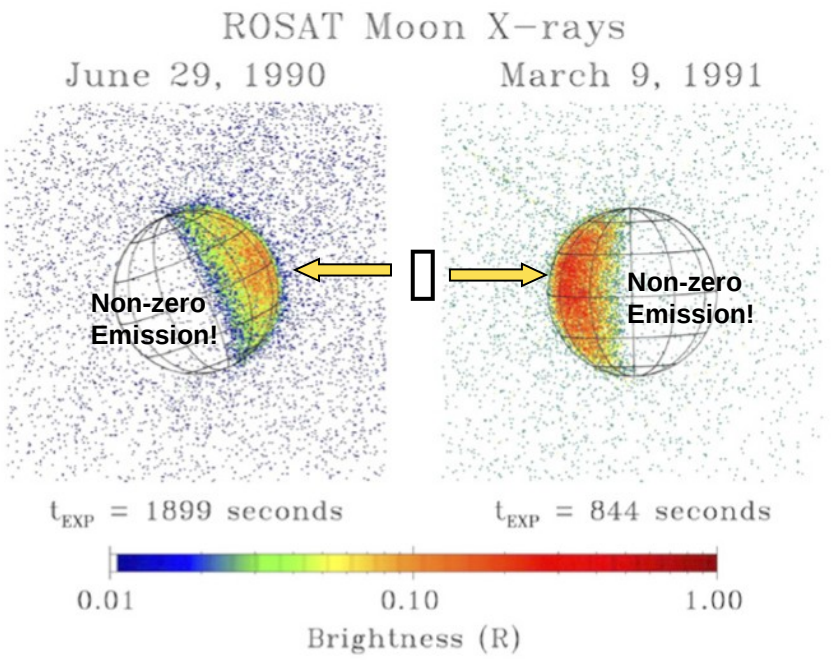

Fig. 9. ROSAT soft X-ray (0.1–2 keV) images of the Moon at first (left side) and last (right side) quarter. The dayside lunar emissions are thought to be primarily reflected and fluoresced sunlight, while the faint night side emissions are foreground due to charge exchange of solar wind heavy ions with H atoms in Earth's exosphere. The brightness scale in R assumes an average effective area of 100 cm^2 for the ROSAT PSPC over the lunar spectrum.

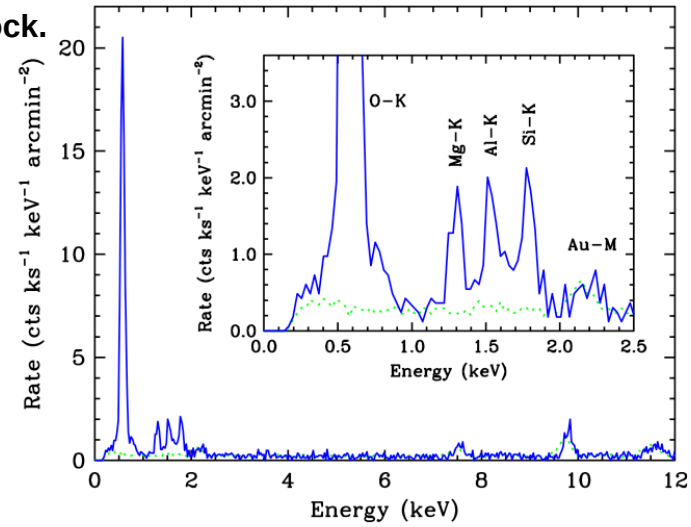

Fig. 10. Chandra spectrum of the bright side of the Moon. The green dotted curve is the detector background. K-shell fluorescence lines from O, Mg, Al, and Si are shifted up by 50 eV from their true values because of residual optical leak effects. Features at 2.2, 7.5, and 9.7 keV are intrinsic to the detector. From Wargelin et al. (2004).

Nightside : ~1% Dayside Rate, Oxygen SWCXE lines.

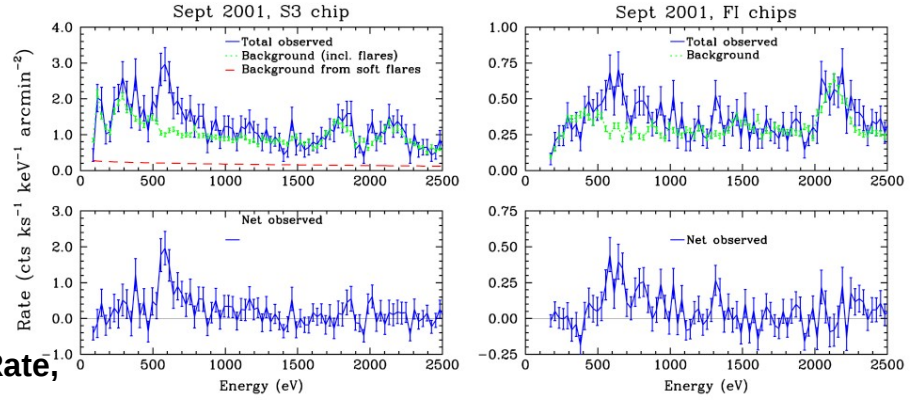

Fig. 14. Observed and background-subtracted spectra from the September 2001 Chandra observation of the dark side of the Moon, with 29-eV binning. Left panel is from the higher-QE but lower-resolution ACIS S3 CCD; right panel shows the higher-resolution ACIS front-illuminated (FI) CCDs. Oxygen emission from charge exchange is clearly seen in both spectra, and energy resolution in the FI chips is sufficient that O Lyman α is largely resolved from O Kα. High-n H-like O Lyman lines are also apparent in the FI spectrum, along with what is likely Mg Kα around 1340 eV. From Wargelin et al. (2004).

FIRST X–RAY IMAGE OF MARS

Dennerl et al. 2002

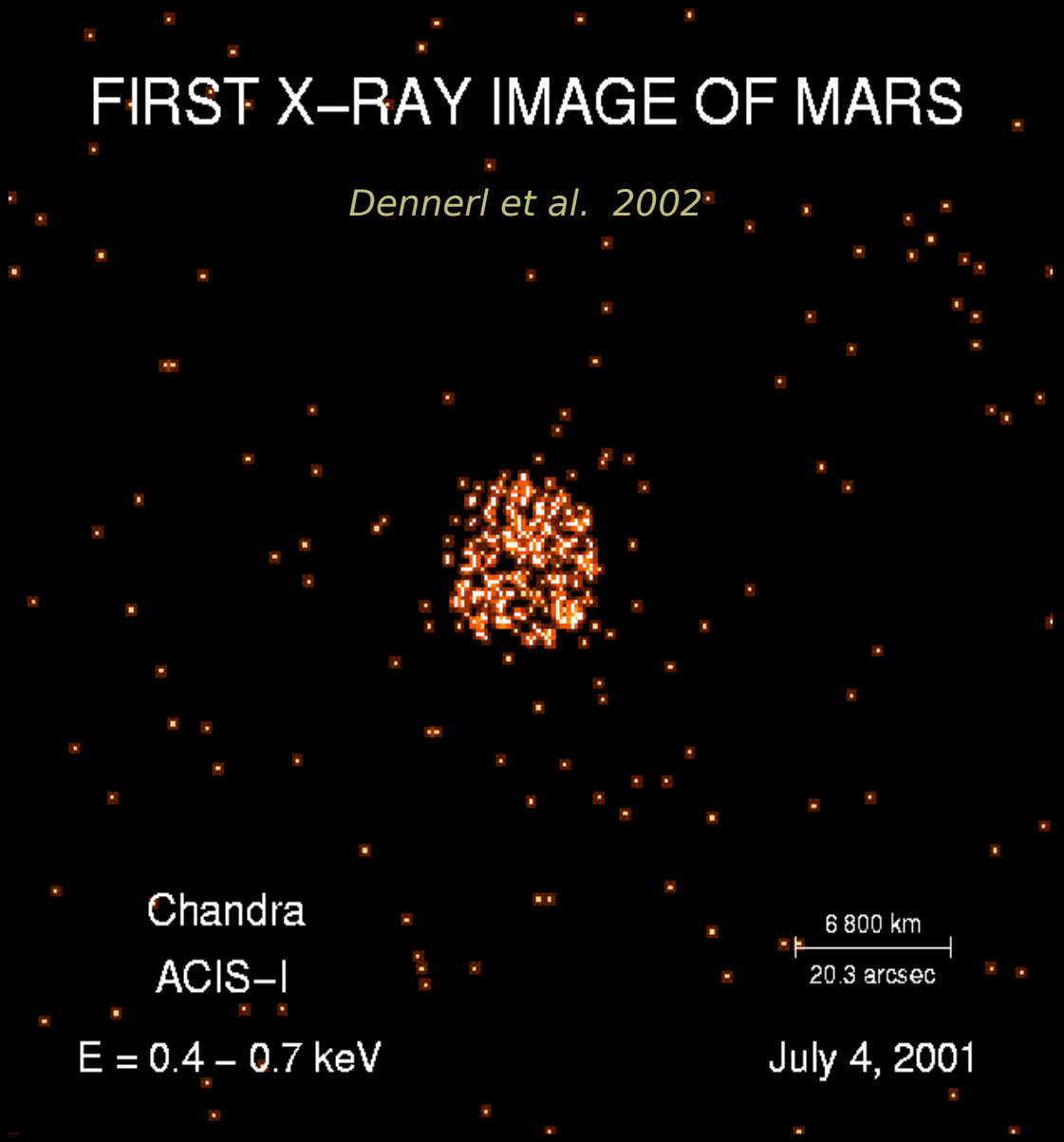

First evidence for exospheric X-ray emission from another planet !

Dennerl 2002

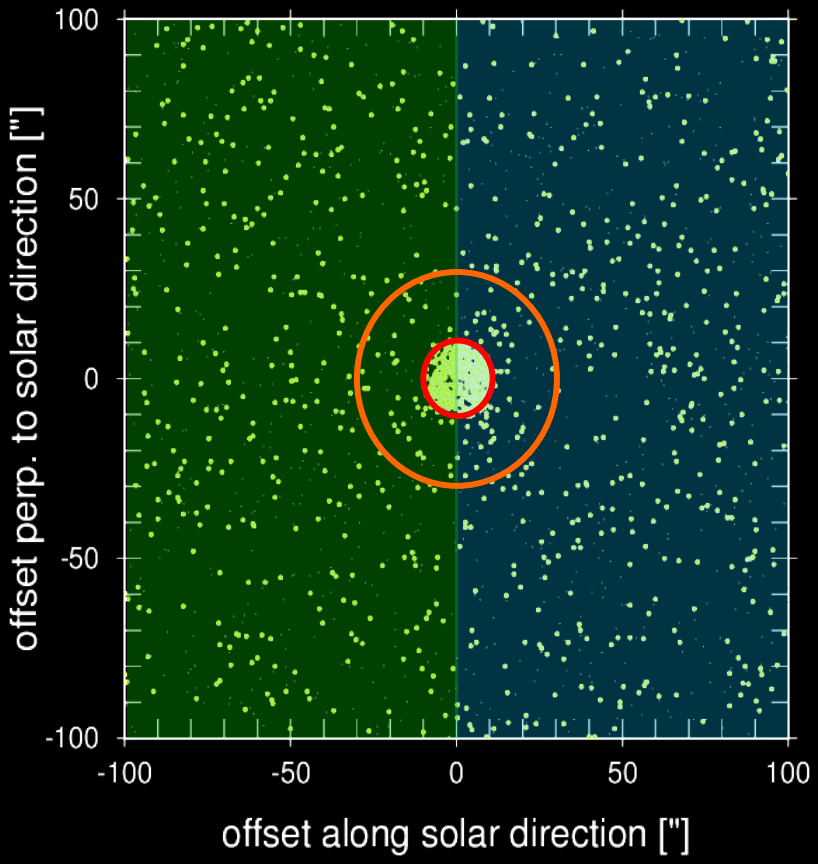

Chandra Observation

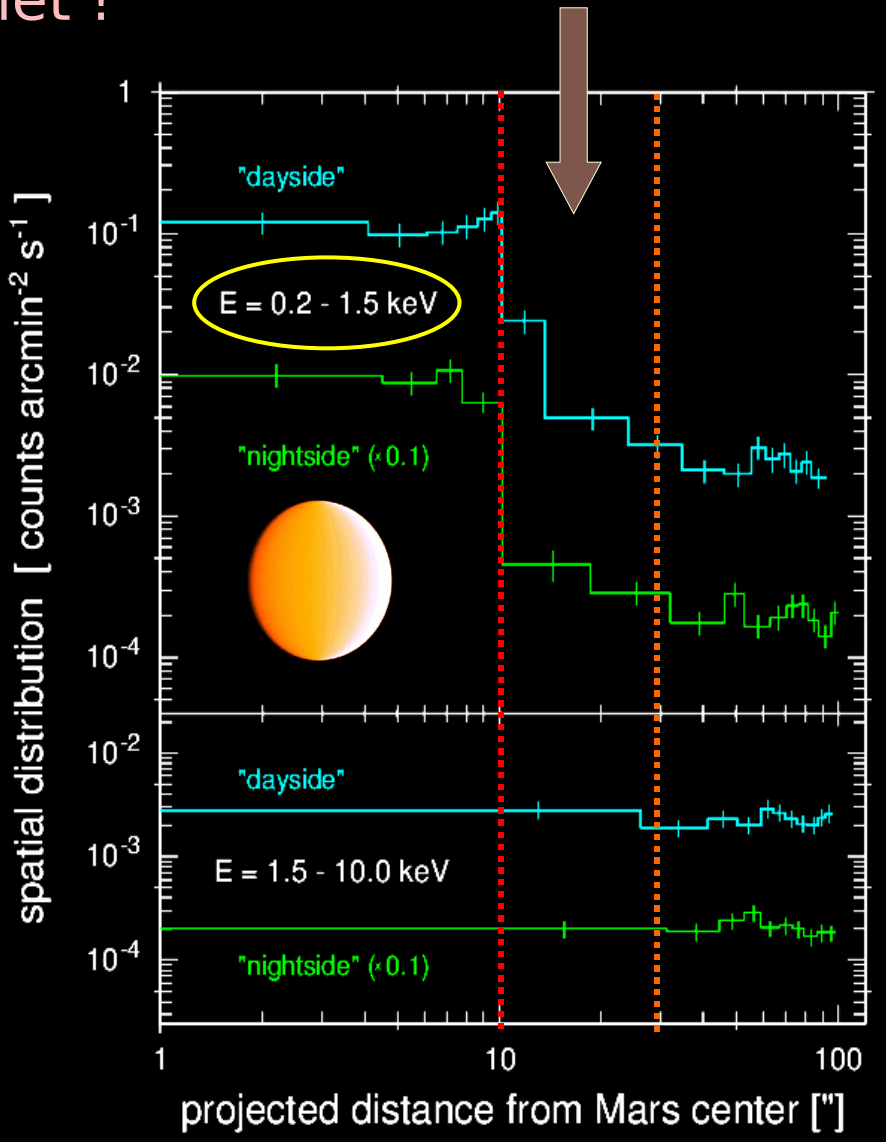

High resolution X-ray spectroscopy of Mars with RGS

Dennerl et al. 2006

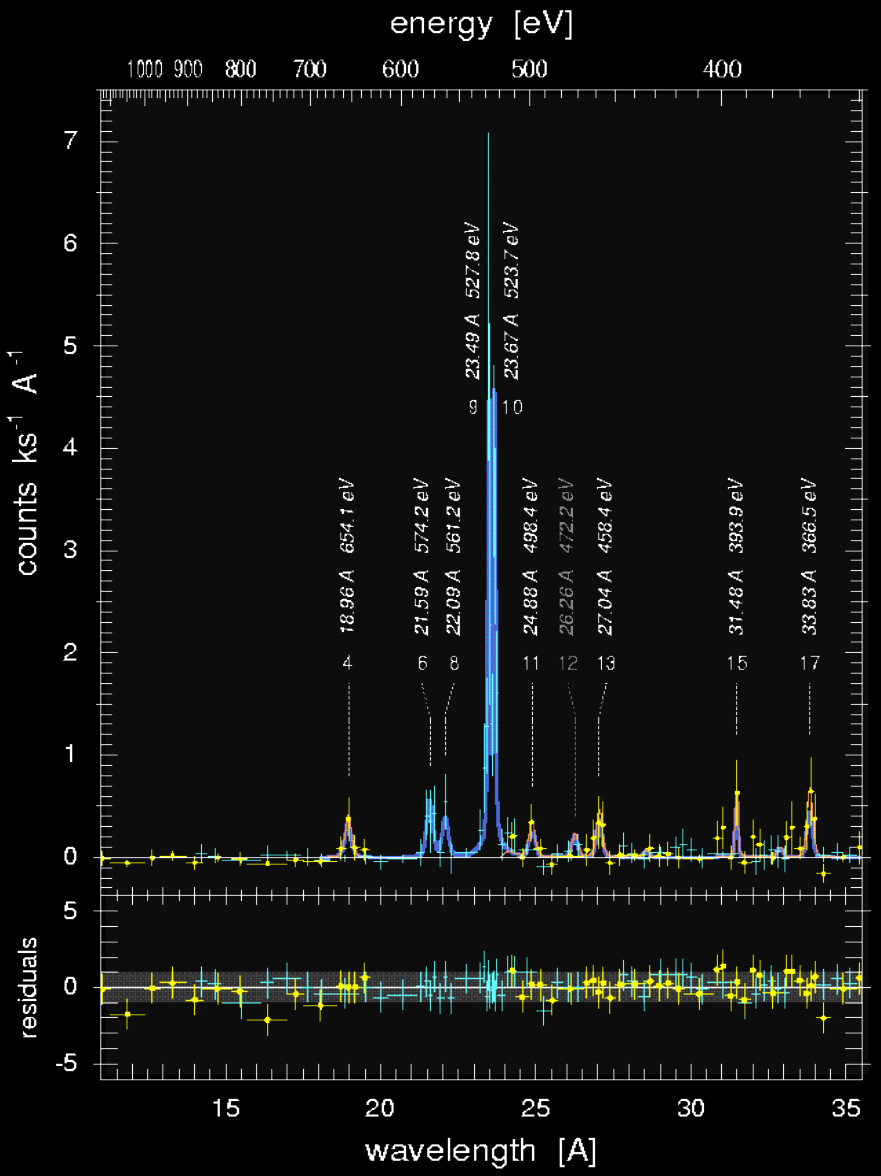

High resolution X-ray spectroscopy of Mars with RGS

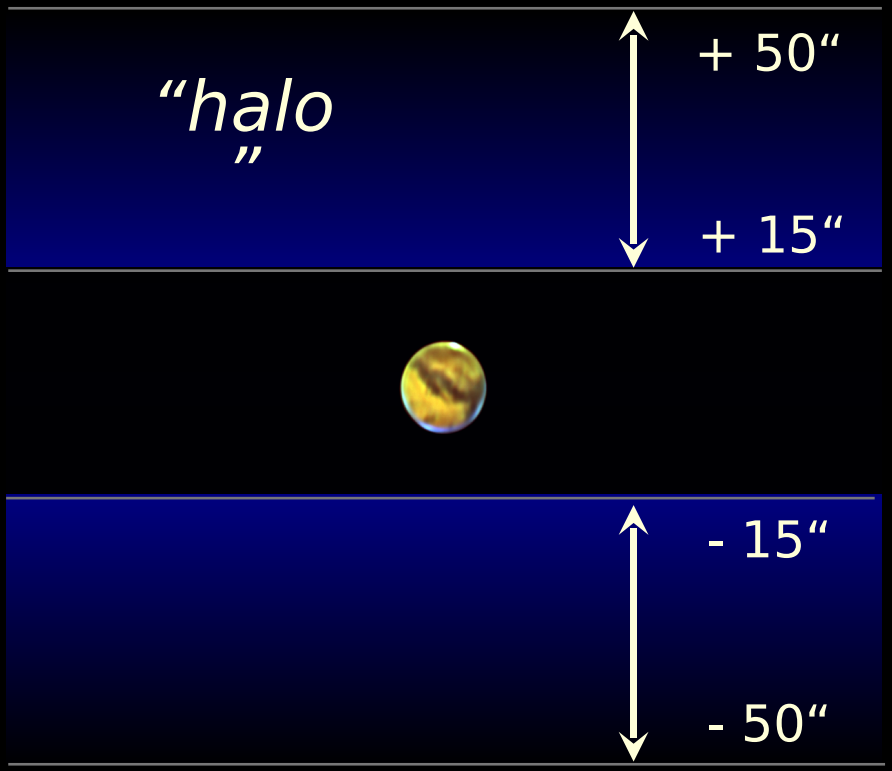

Dennerl et al. 2006

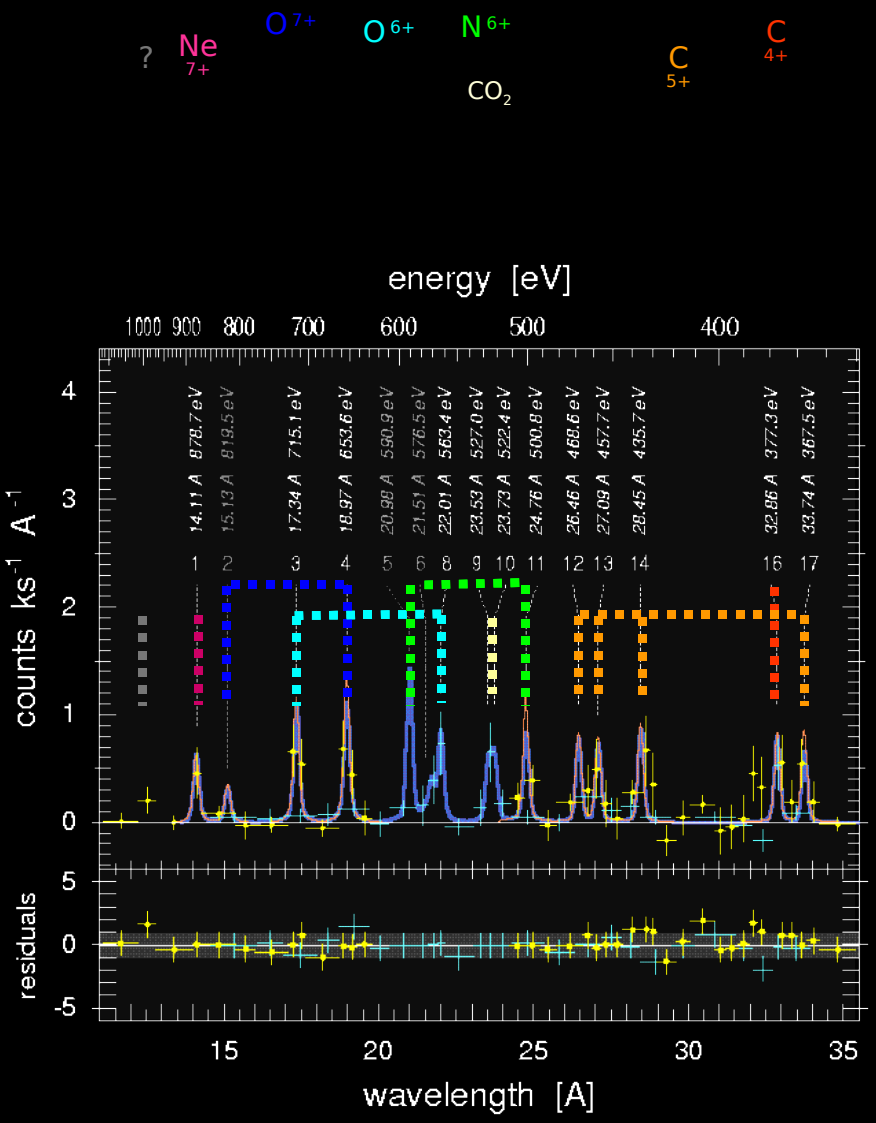

X-ray images of Mars in individual emission lines (!)

fluorescence

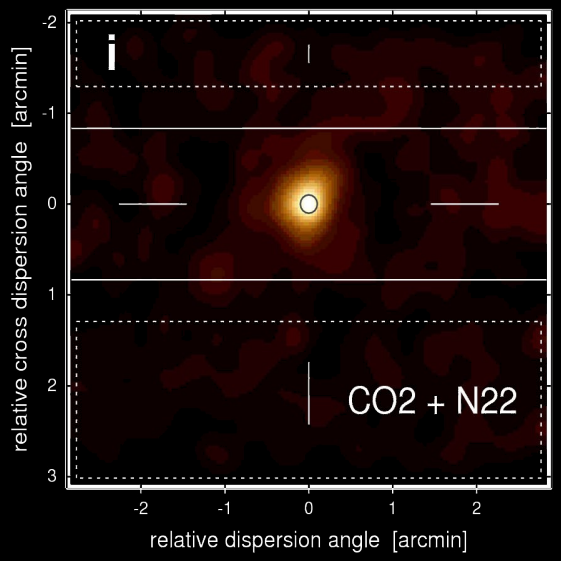

Emission centered on disk.

ionized carbon

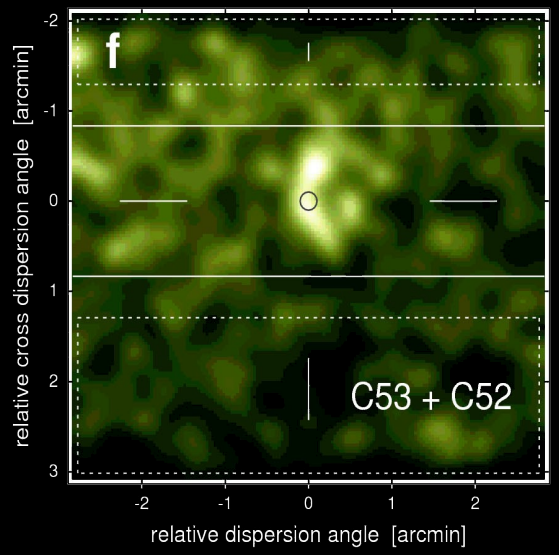

Emission in crescent offset towards the Sun.

ionized oxygen

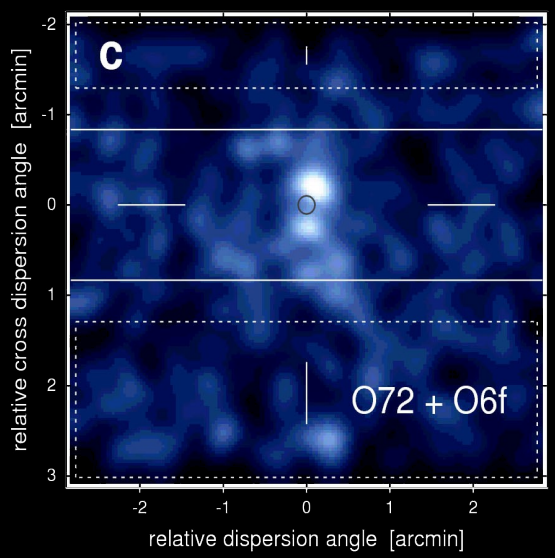

Emission above and below Poles (!?) or in limb-effect crescent.

Alas, no obvious variation of x-ray signal in/out of hemisphere covering dust storm.

January 2001: first X-ray image of Venus (Chandra ACIS-I)

First X-ray observation of Venus during solar maximum: **Scattering of solar X-rays detected, but no conclusive evidence of charge exchange.**

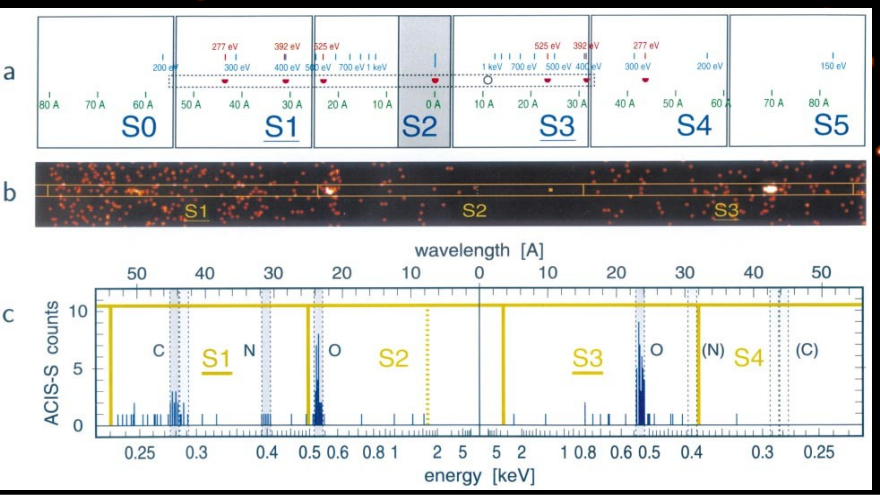

Dennerl et al. 2002, *A&A* **386,** 319

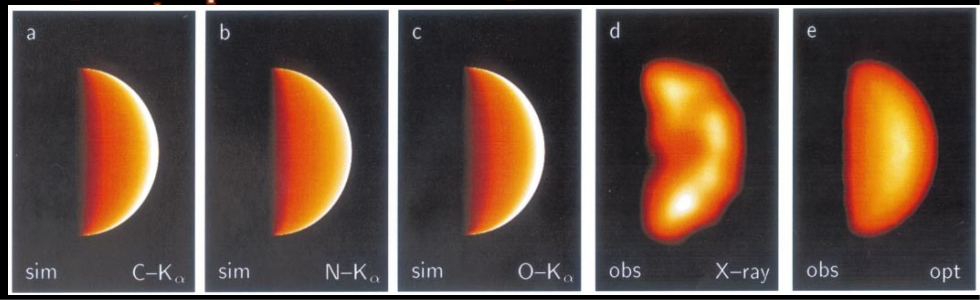

X-ray grating spectrum of Venus (Chandra LETG/ACIS-S)

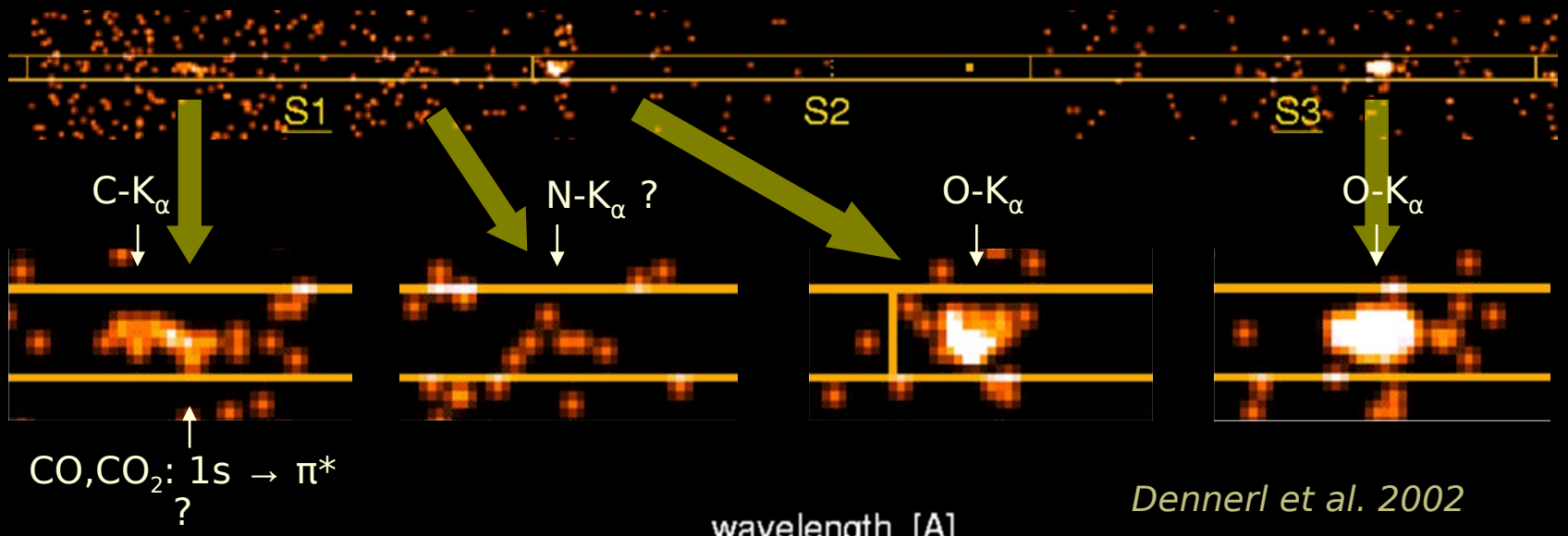

Dennerl et al. 2002

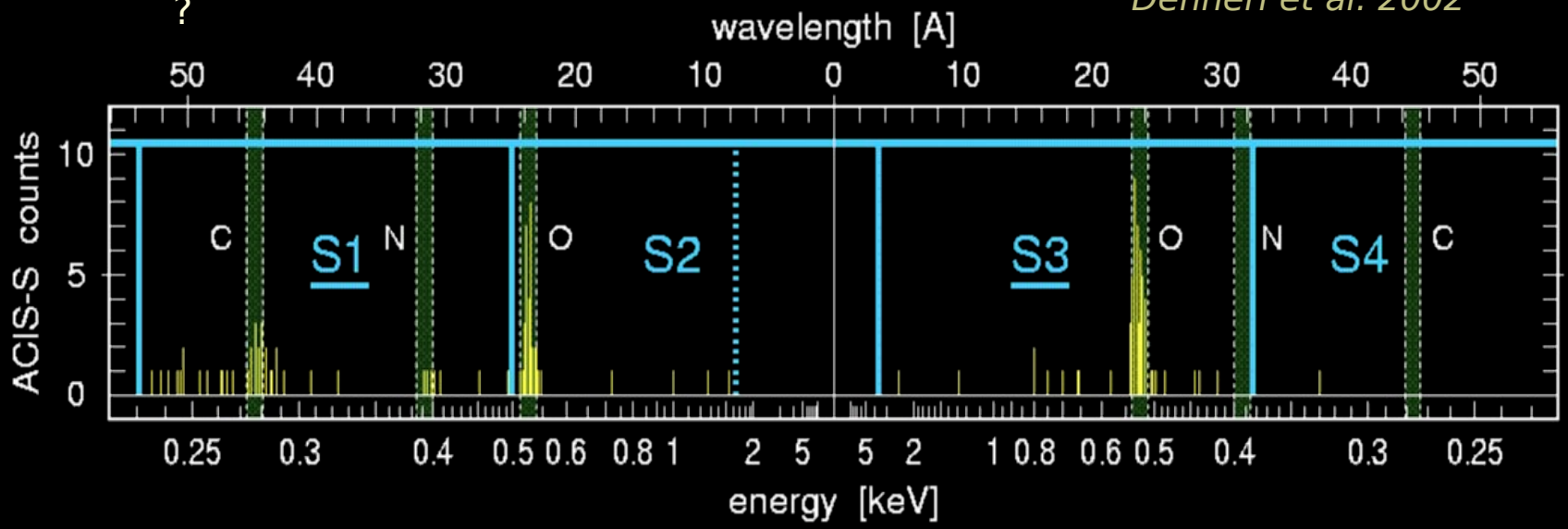

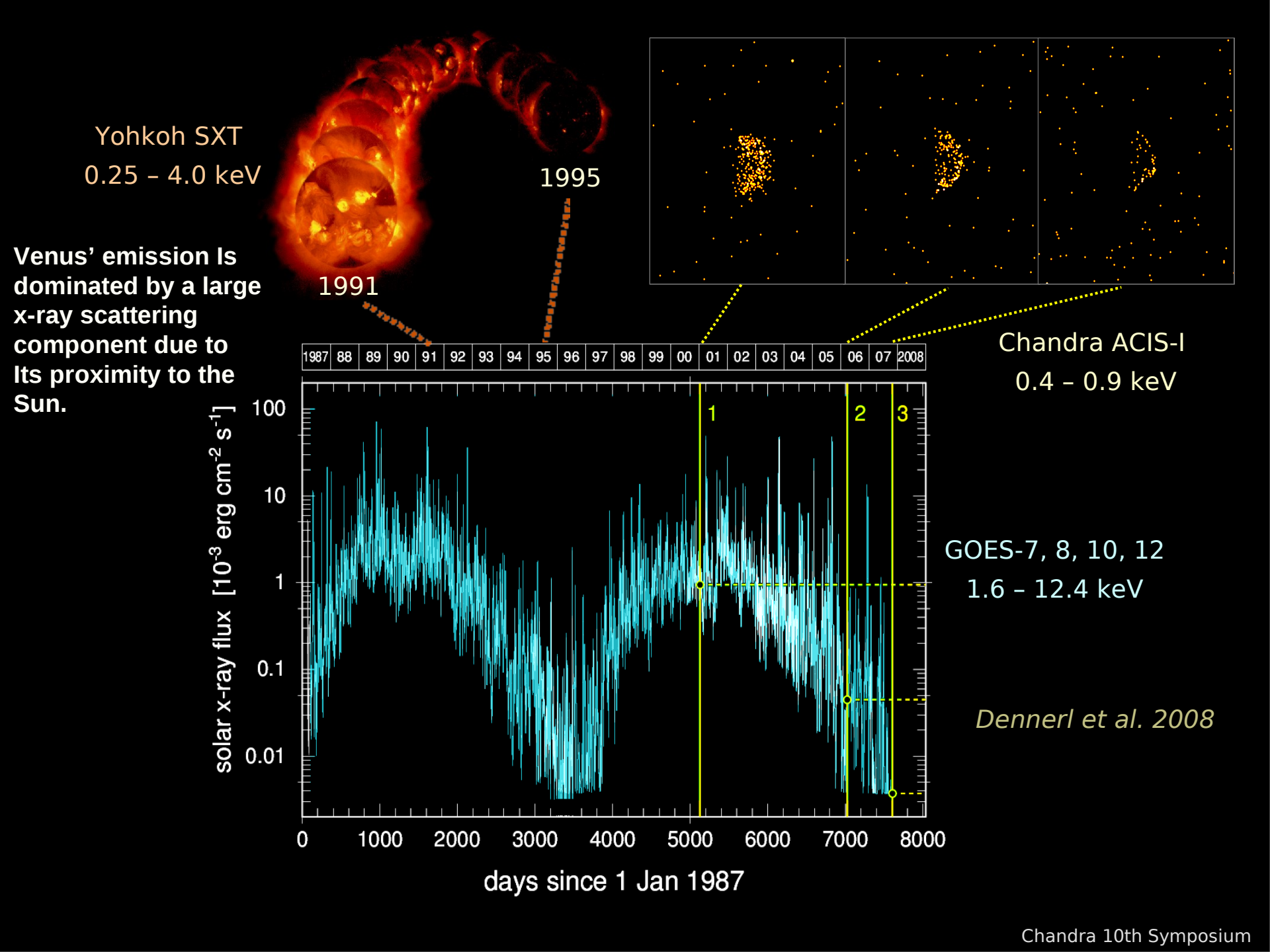

Venus' emission Is dominated by a large x-ray scattering component due to Its proximity to the Sun.

Second Chandra observation of Venus, 2006 March 27 (ACIS-S, 74.9 ks)

First evidence for exospheric X-ray emission from Venus !

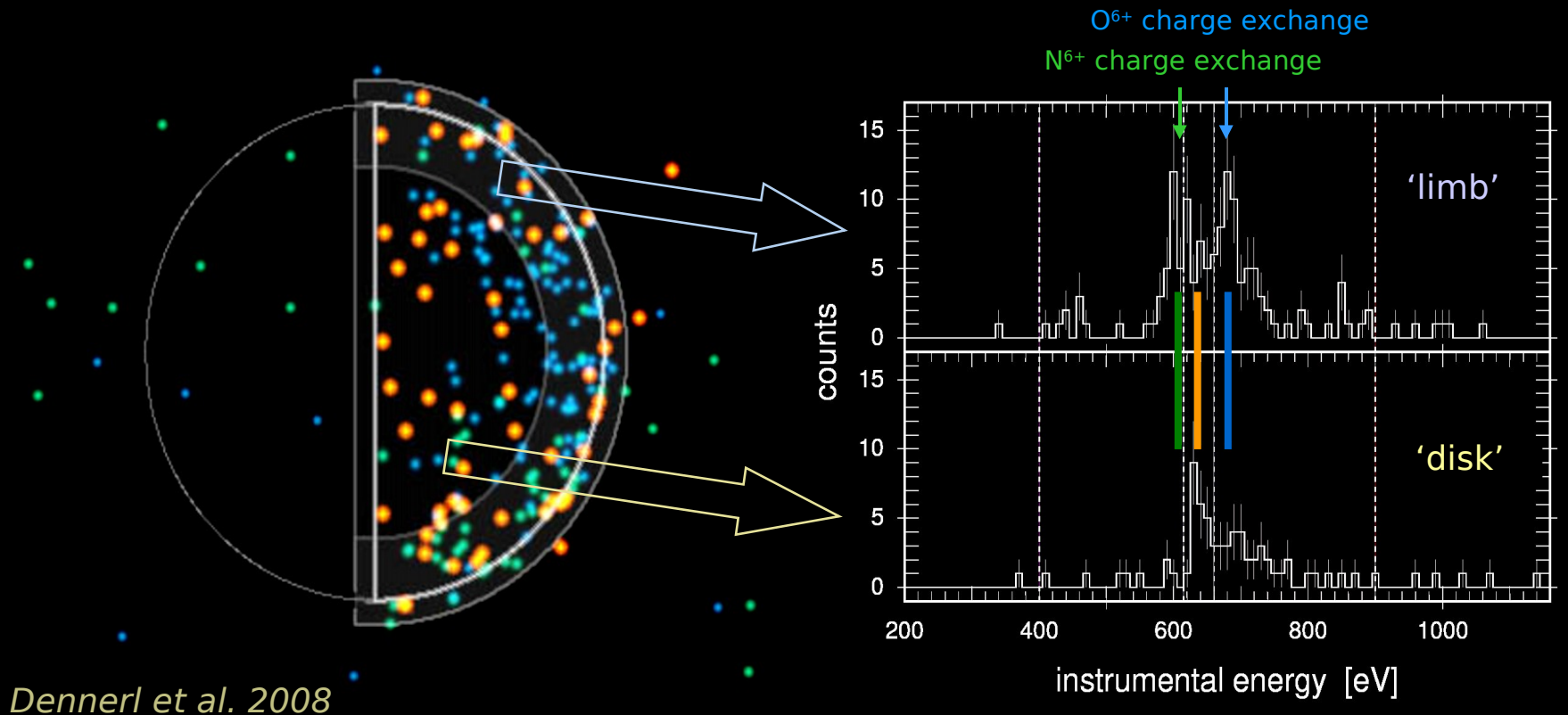

Dennerl et al. 2008

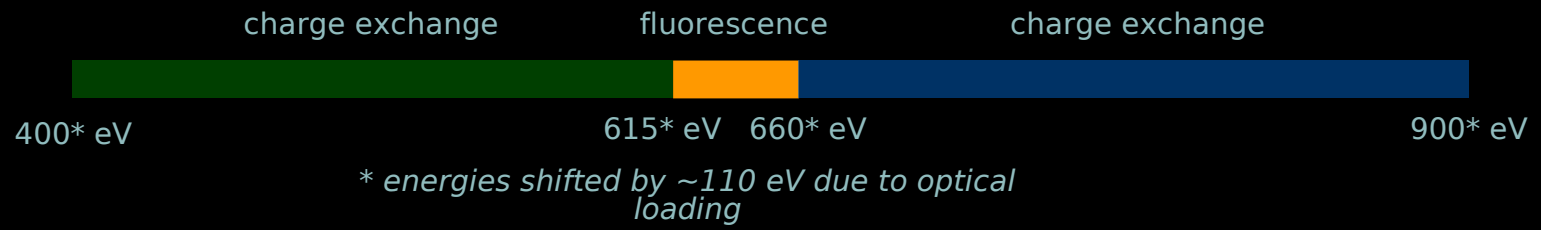

** energies shifted by ~110 eV due to optical loading*

Jovian X-rays : Disk Scattering of Solar X-rays + Auroral Precipitation + Polar SWCX

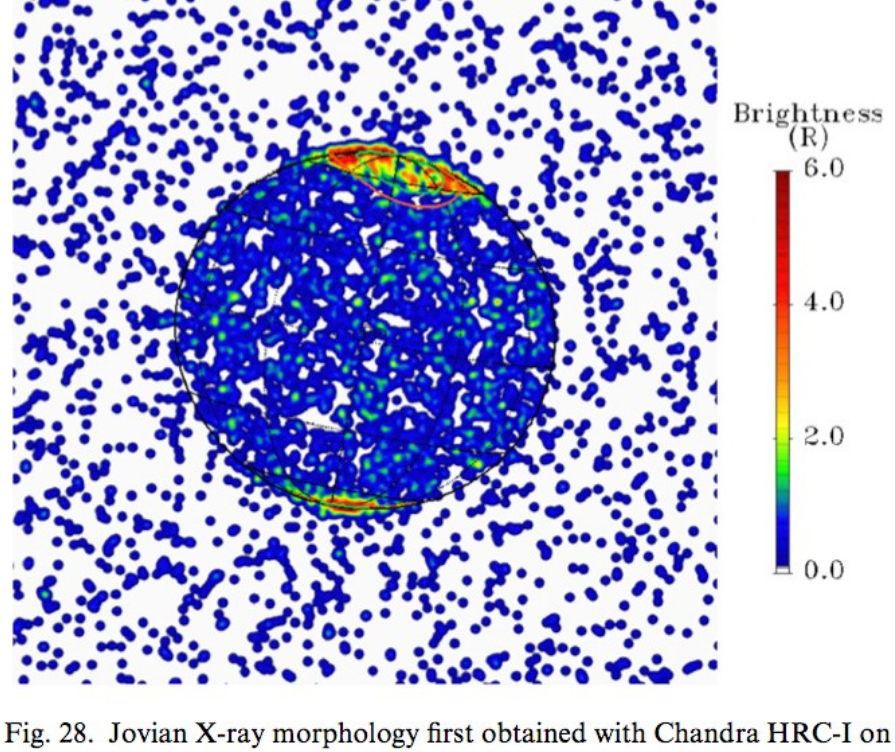

Fig. 28. Jovian X-ray morphology first obtained with Chandra HRC-I on 18 December 2000, showing bright X-ray emission from the polar 'auroral' spots, indicating the high-latitude position of the emissions, and a uniform distribution from the low-latitude 'disk' regions (from Gladstone et al., 2002).

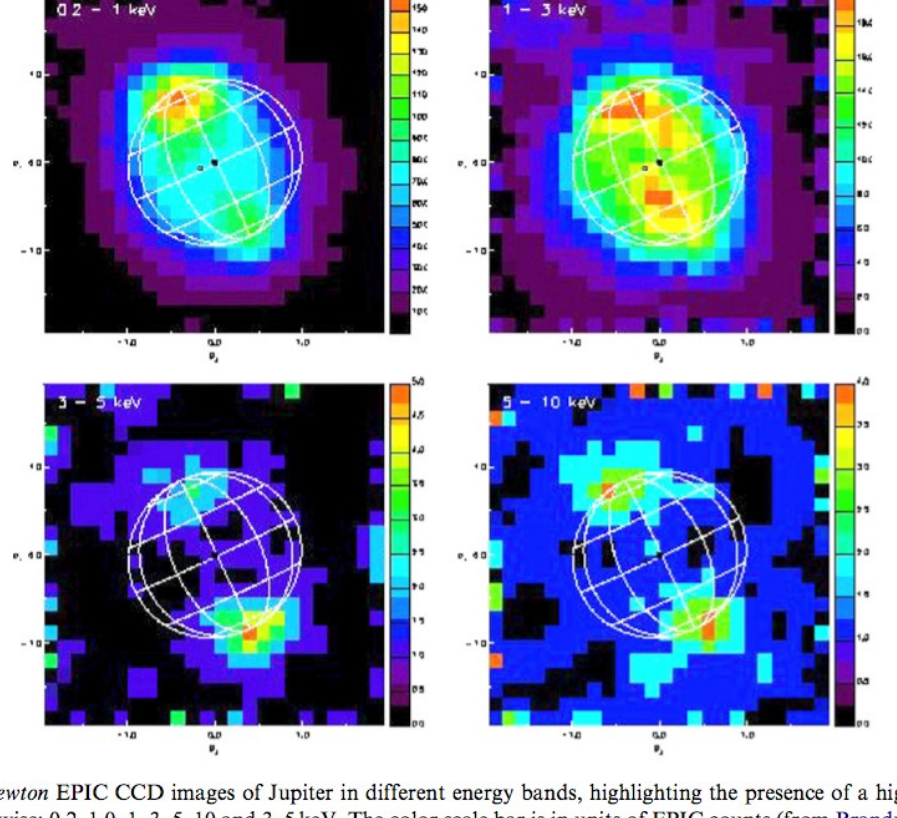

M-Newton EPIC CCD images of Jupiter in different energy bands, highlighting the presence of a high en clockwise: 0.2–1.0, 1–3, 5–10 and 3–5 keV. The color scale bar is in units of EPIC counts (from Branduard

Jovian Disk X-rays Correlate With Solar X-ray Output…

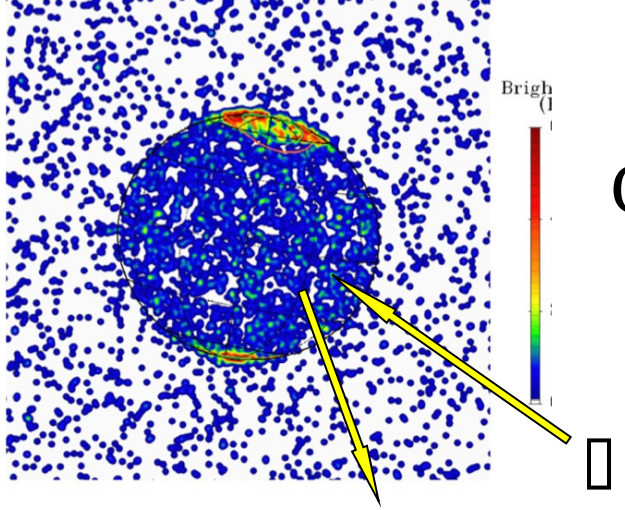

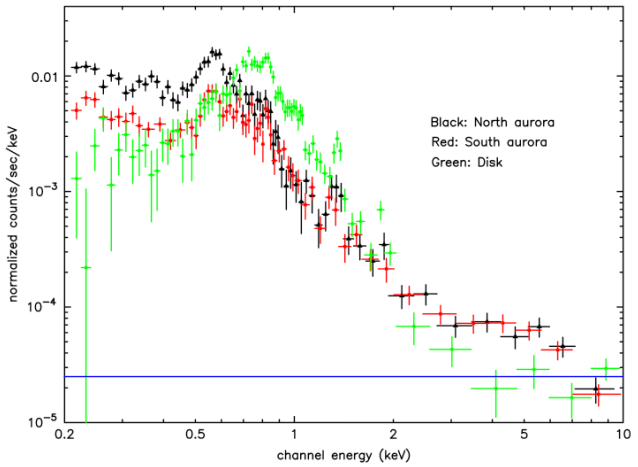

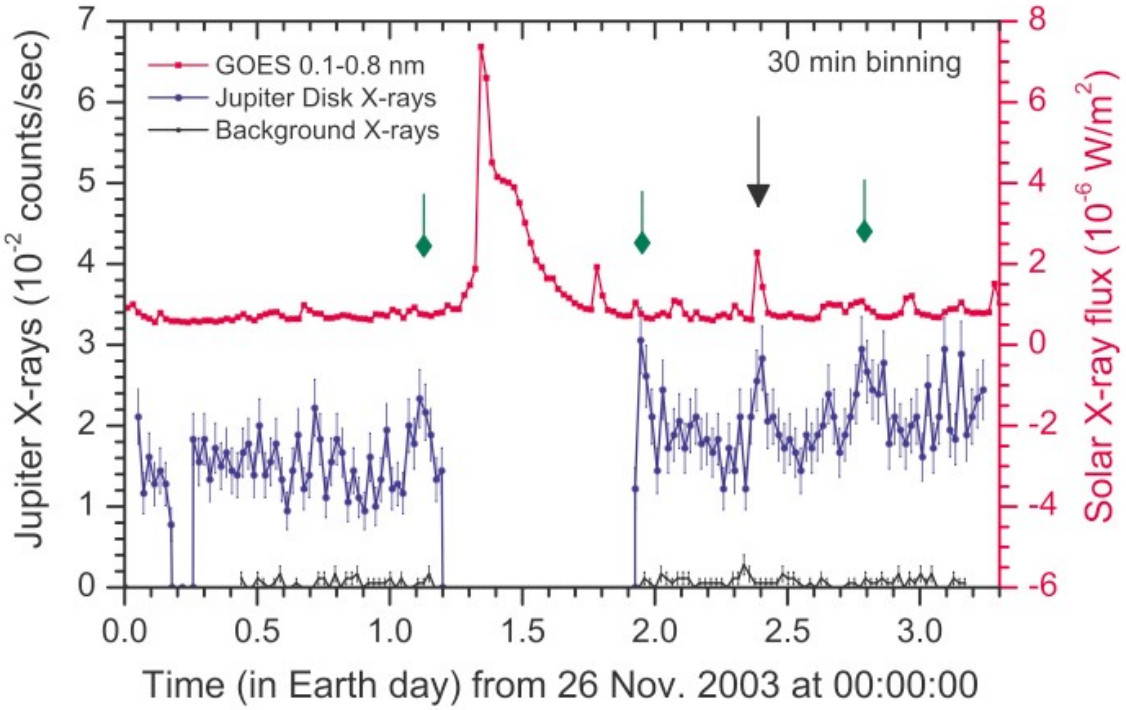

Fig. 30. Comparison of Jupiter's disk X-ray lightcurve in November 2003 (blue) with GOES 10 0.1–0.8 nm solar X-ray data (red), after shifting to account for light travel time delay. The black arrow (at 2.4 days) refers to the time of the largest solar flare visible from both, Earth and Jupiter (from Bhardwaj et al., 2005a).

…and the Polar X-ray Spectrum can be fit by a Combination of Io's O and S undergoing CXE (no solar wind C!)…at an Unexpected Polar Location.

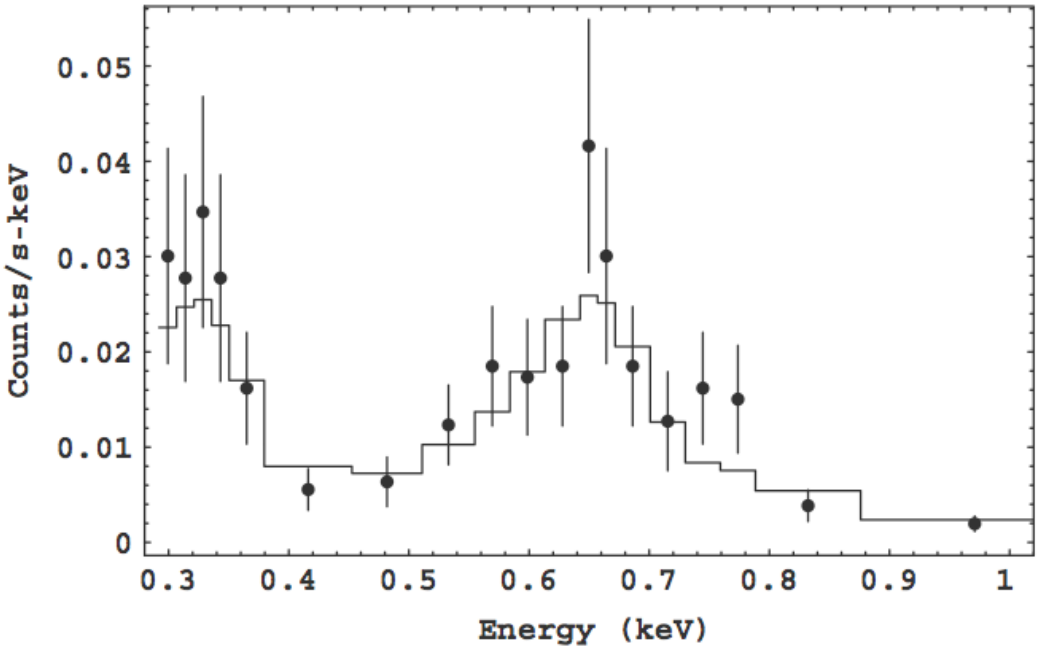

Fig. 24. Fit with 2 added VAPEC models of the north auroral zone emission between 300 eV and 1 keV.The fitting parameters are the plasma temperature of oxygen and sulfur, the ratio of sulfur over oxygen and a normalization factor. Vapec model consider a species in collisional equilibrium. The χ^2 is 11.51, the reduced chi-squared is 0.767. S/O is 16.6 times the solar value, the oxygen temperature is 355 eV and the sulfur temperature is 172 eV (from Elsner et al., 2005a).

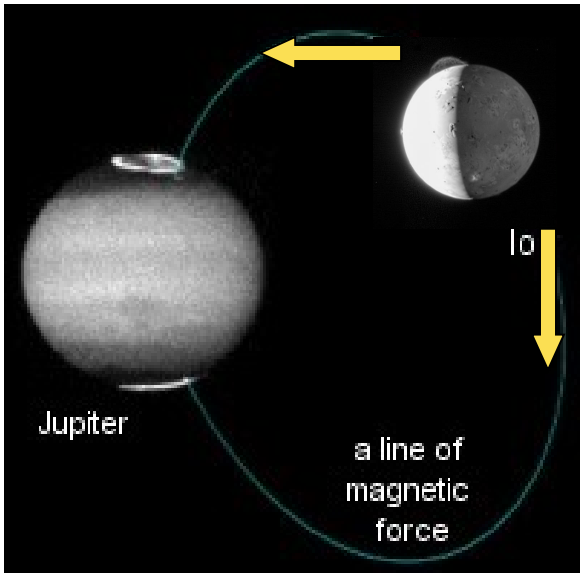

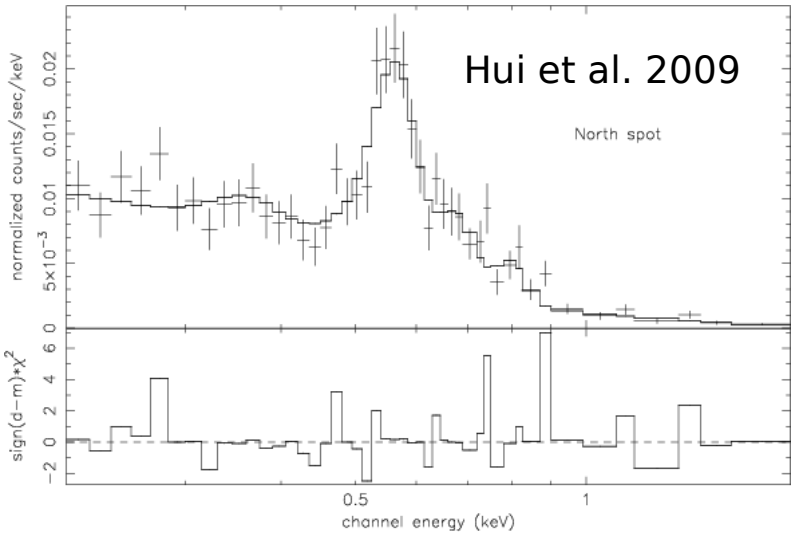

Jovian UV and X-ray Emission are Coupled? Footprints are off.

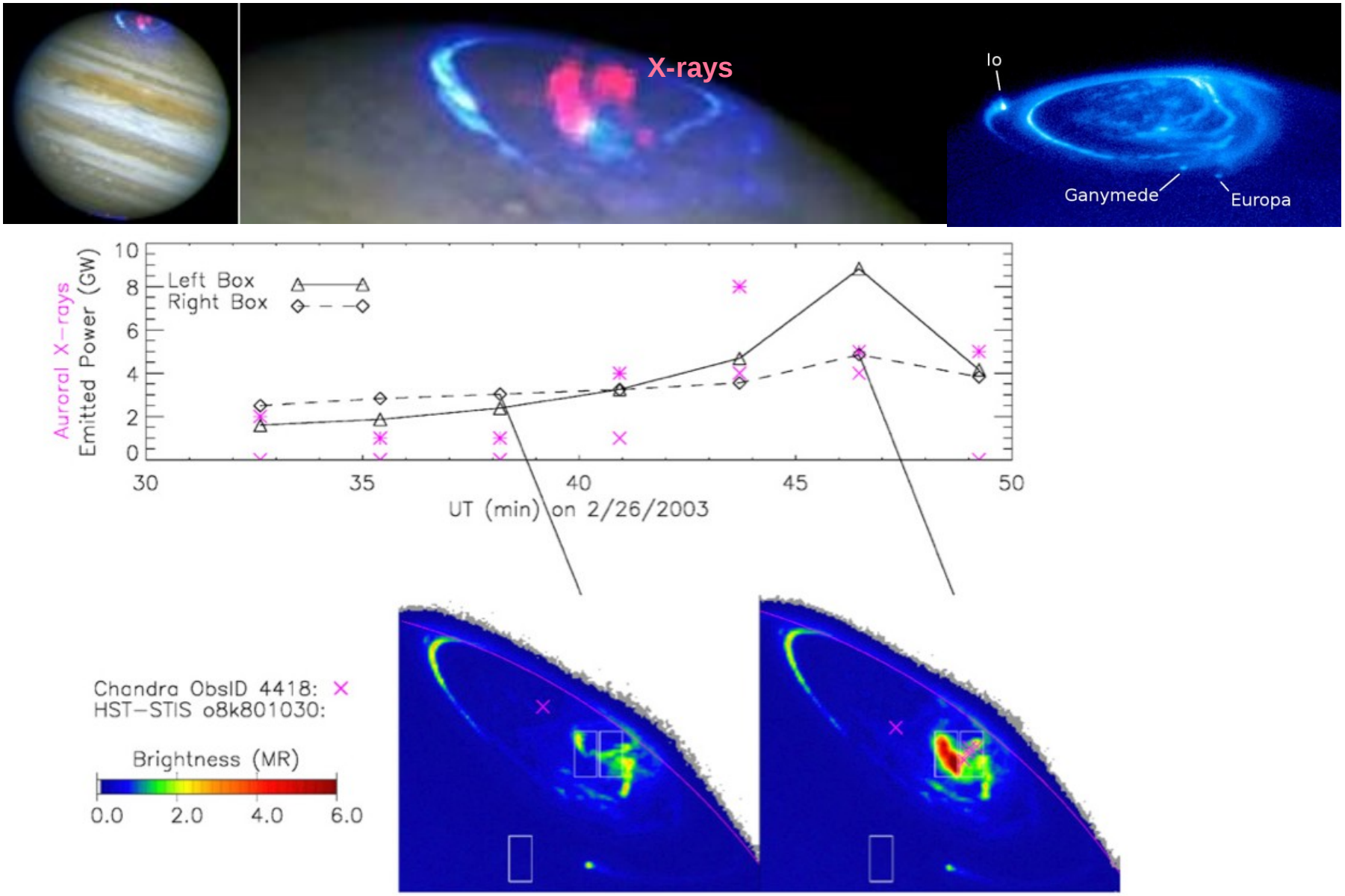

The relationship between ultraviolet emission and X-ray emission in a bright Jovian polar flare (from Elsner et al., 2005a).

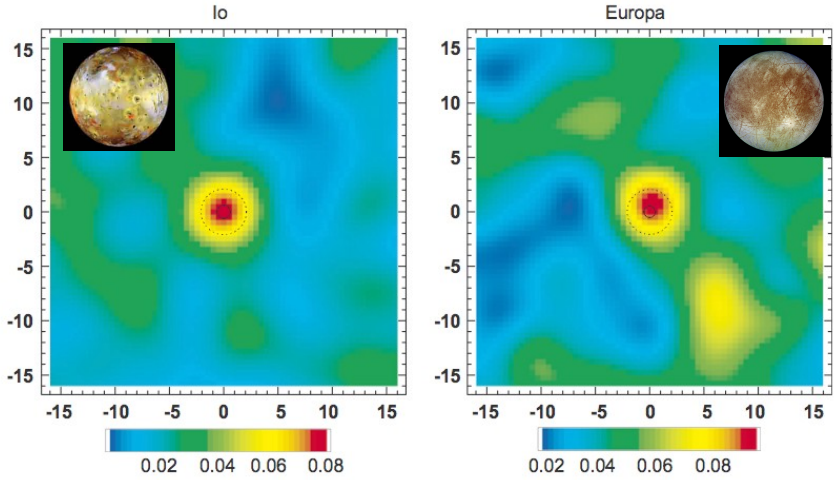

Fig. 41. CXO images of Io and Europa (0.25 keV < E < 2.0 keV) from November 1999 (Elsner et al. 2002). The images have been smoothed by a two-dimensional gaussian with $\sigma = 2.46$ arcsec (5 detector pixels). The axes are labeled in arcsec (1 arcsec $\sim = 2995$ km) and the scale bar is in units of smoothed counts per image pixel (0.492 × 0.492 arcsec). The solid circle shows the size of the satellite (the radii of Io and Europa are 1821 and 1560 km, respectively), and the dotted circle the size of the detect cell (from Elsner et al., 2002).

Io, Europa, Ganymede, and the *Io Plasma Torus* have been detected in the X-ray.

Does the *IPT* provide the S, O atoms for Jupiter's Polar X-ray emission?

Have we detected the root of *Europa's Neutral Atom Torus* (Mauk *et al.* 2003)?

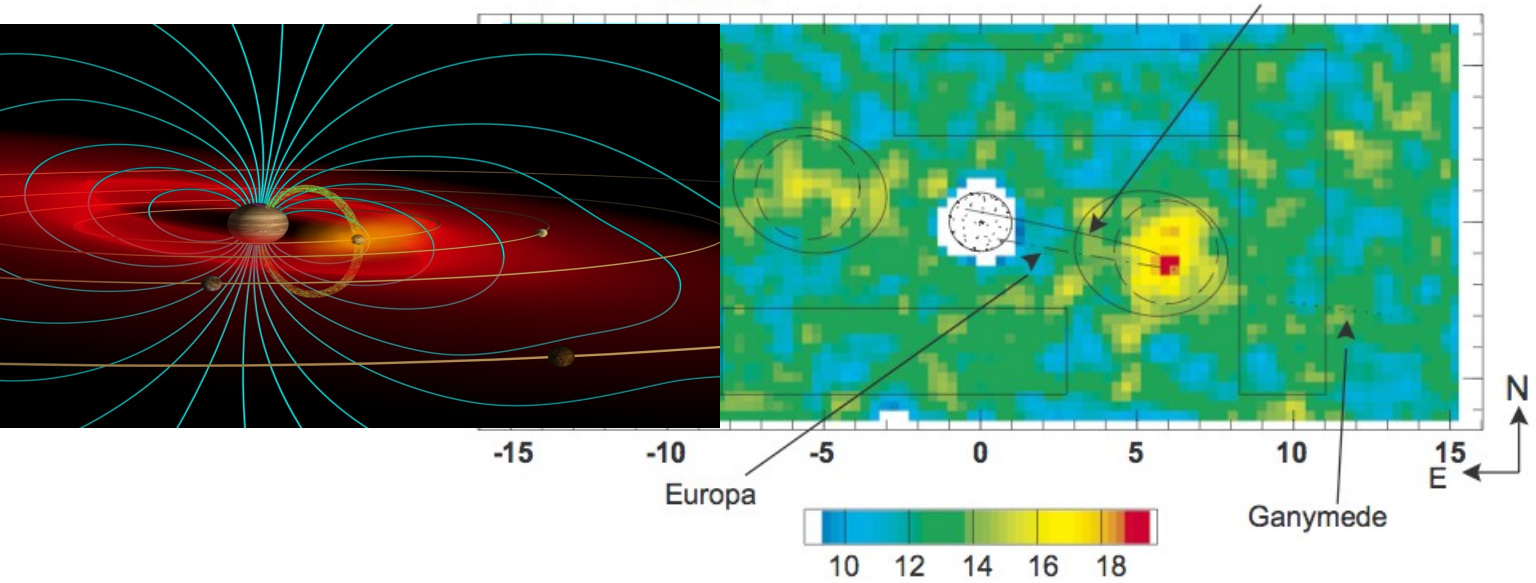

Fig. 39. Chandra/HRC-I image of the IPT (2000 December 18). The image has been smoothed by a two-dimensional Gaussian with $\sigma = 7.38''$ (56 HRC-I pixels). The axes are labeled in units of Jupiter's radius, R_J, and the scale bar is in units of smoothed counts per image pixel. The paths traces by Io, Europa, and Ganymede are marked on the image. Callisto is off the image to the dawn side, although the satellite did fall within the full microchannel plate field of view. The regions bounded by rectangles were used to determine background. The regions bounded by dashed circles or solid ellipses were defined as source regions (from Elsner et al., 2002).

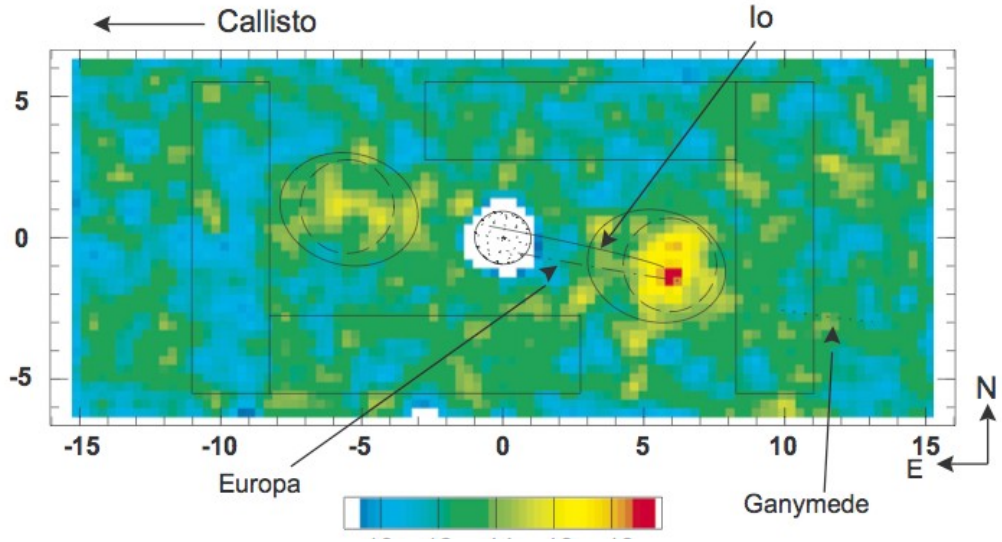

The IPT Appears to Glow in Oxygen Kα Fluorescence. Where's the Sulfur Kα?

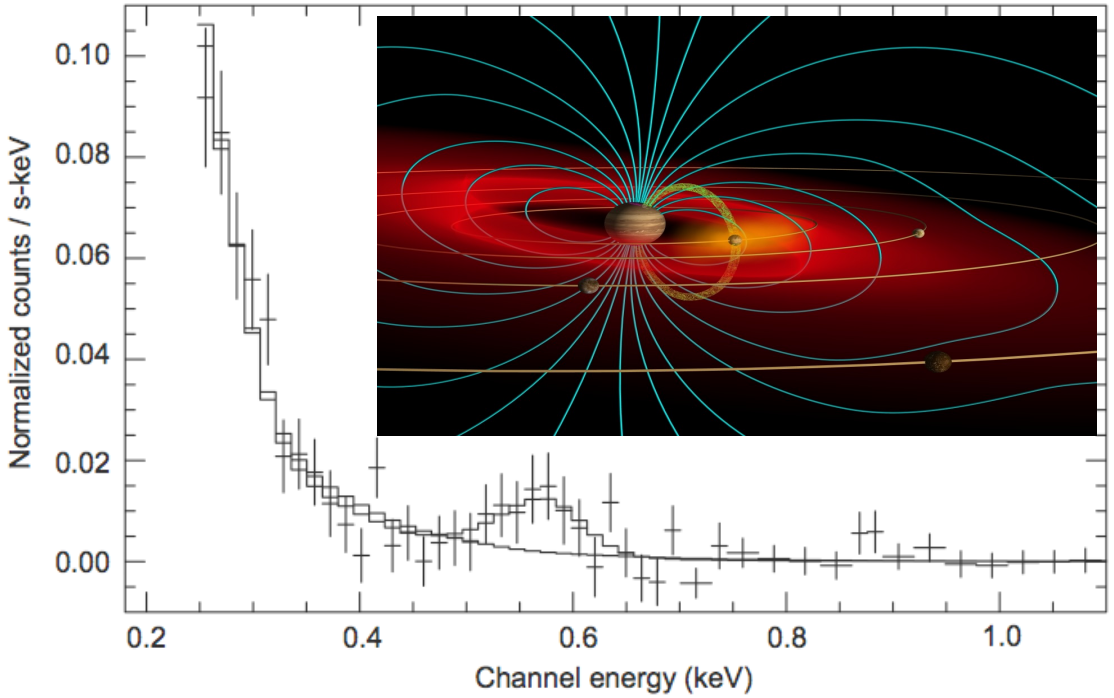

Fig. 40. Chandra/ACIS-S spectrum for the Io Plasma Torus from November 1999. The solid line presents a model fit for the sum of a power-law spectrum and a Gaussian line, while the dashed line represents just a pure power law spectrum. The line is consistent with K-shell flurorescent emission from oxygen ions (from Elsner et al., 2002).

Saturn

RADIO INFRARED OPTICAL ULTRAVIOLET

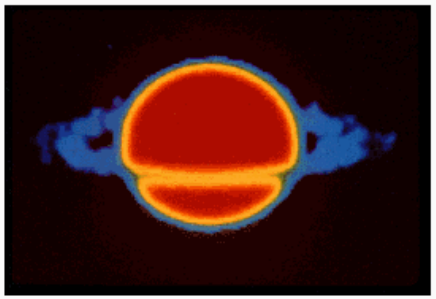

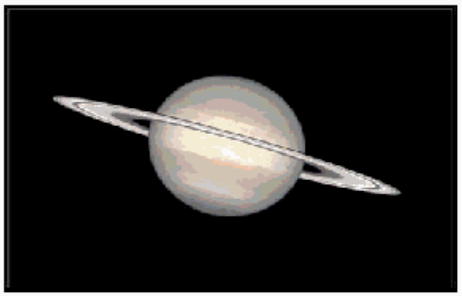

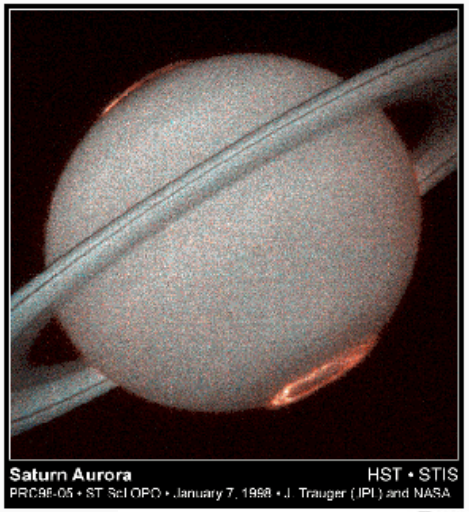

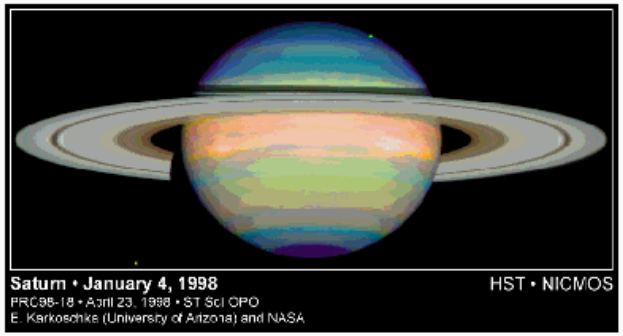

…X-ray (w/ high variability and polar enhancement [but no definite evidence of auroral emission yet]). Bhardwaj *et al.* 2005

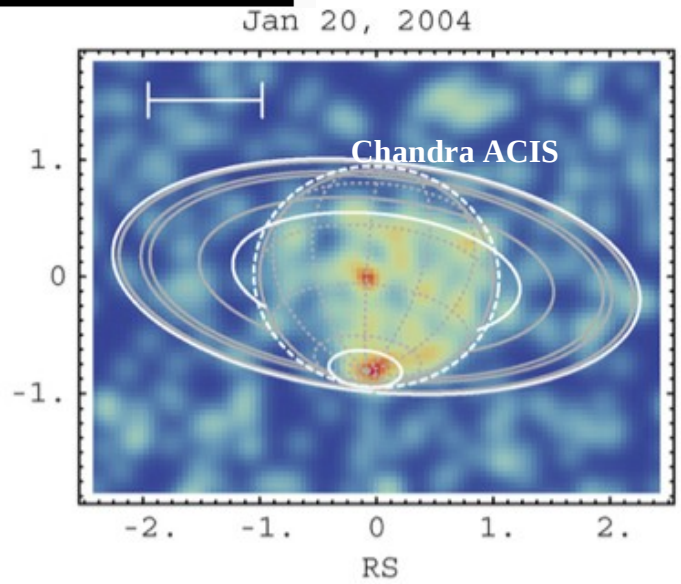

Saturn's X-ray Lightcurve Follows the Sun's Closely (Much More Than Jupiter)

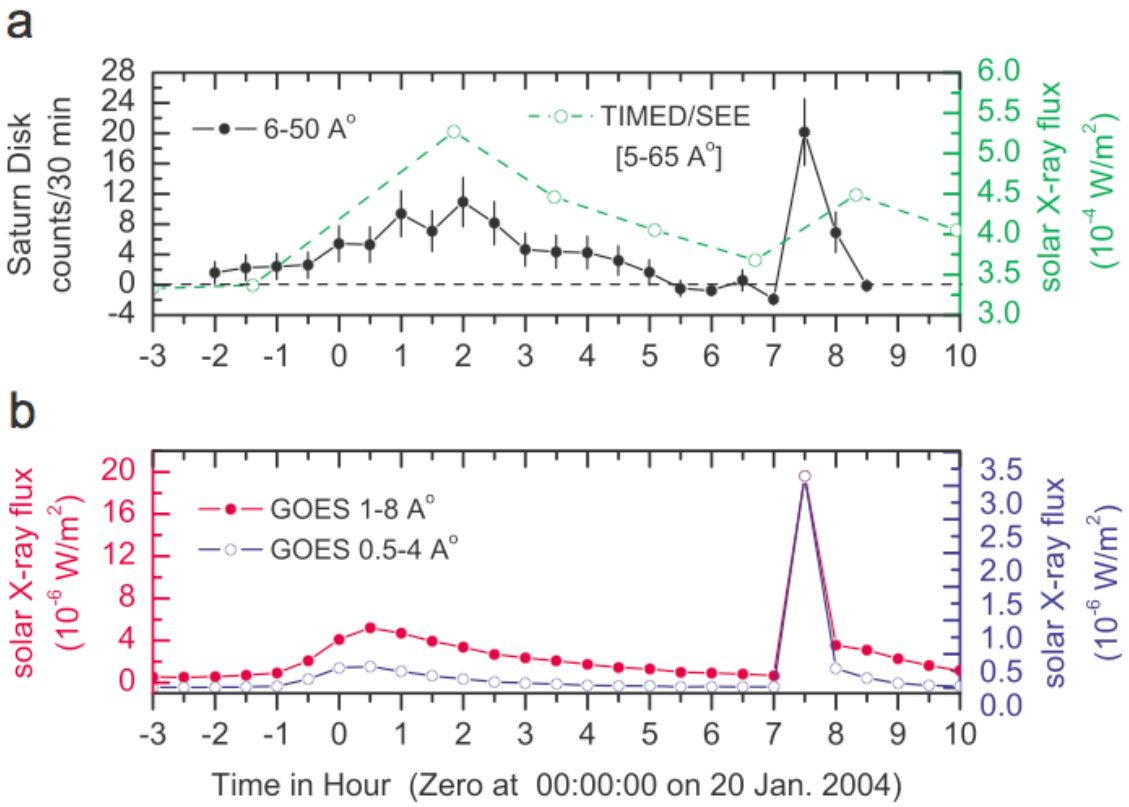

Fig. 32. Light curve of X-rays from Saturn and the Sun on 2004 January 20. All data are binned in 30-min increments, except for the TIMED/SEE data, which are 3 min observation-averaged fluxes obtained every orbit (~12 measurements per day). (a) Background-subtracted low-latitude (nonauroral) Saturn disk X-rays (0.24–2.0 keV) observed by Chandra ACIS, plotted in black (after shifting by −2.236 h to account for the light-travel time difference between Sun–Saturn–Earth and Sun–Earth). The solar 0.2–2.5 keV fluxes measured by TIMED/SEE are denoted by open green circles and are joined by the green dashed line for visualization purpose. (b) Solar X-ray flux in the 1.6–12.4 and 3.1–24.8 keV bands measured by the Earth-orbiting GOES-12 satellite. A sharp peak in the light curve of Saturn's disk X-ray flux—an X-ray flare—is observed at about 7.5 h, which corresponds in time and magnitude with an X-ray solar flare. In addition, the temporal variation in Saturn's disk X-ray flux during the time period prior to the flare is similar to that seen in the solar X-ray flux (from Bhardwaj et al., 2005b).

Saturn's Rings Shine in Oxygen Kα Fluorescence

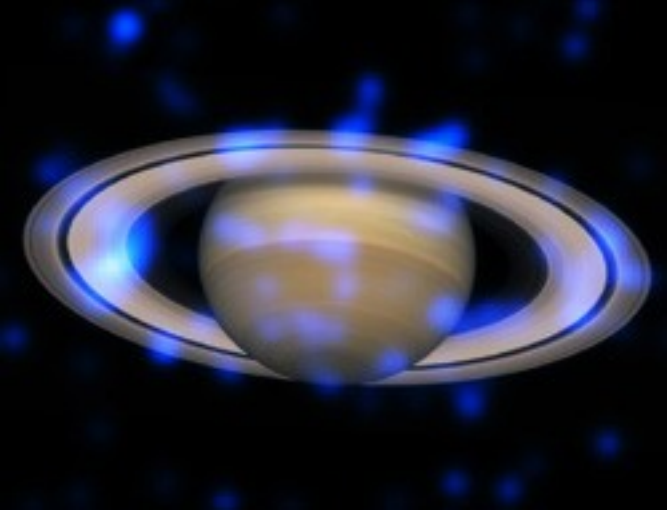

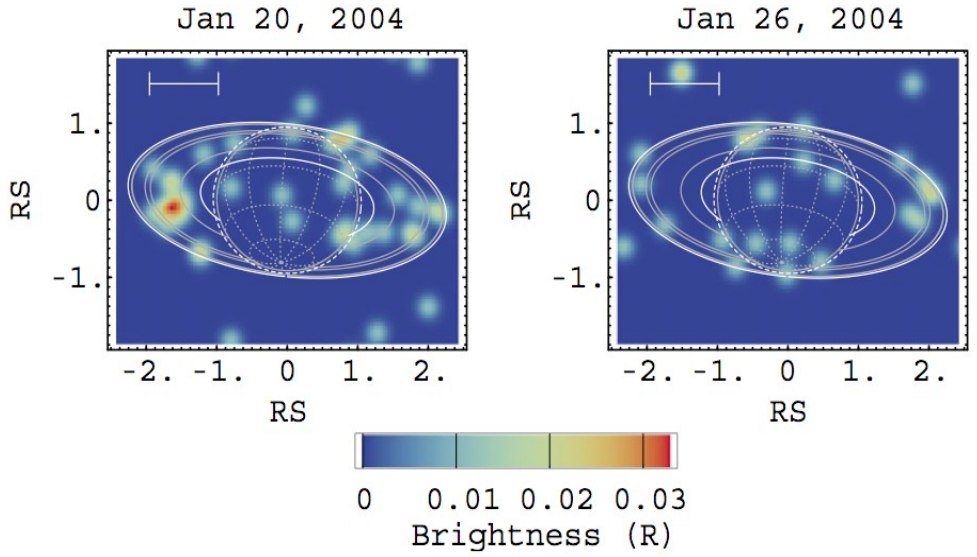

Fig. 43. Chandra ACIS X-ray images of the Saturnian system in the 0.49–0.62 keV band on 2004 January 20 and 26–27. The X-ray emission from the rings is clearly present in these restricted energy band images (see Fig. 42); the emission from the planet is relatively weak in this band (see Fig. 31 for an X-ray image of the Saturnian system in the 0.24–2.0 keV band) (from Bhardwaj et al., 2005c).

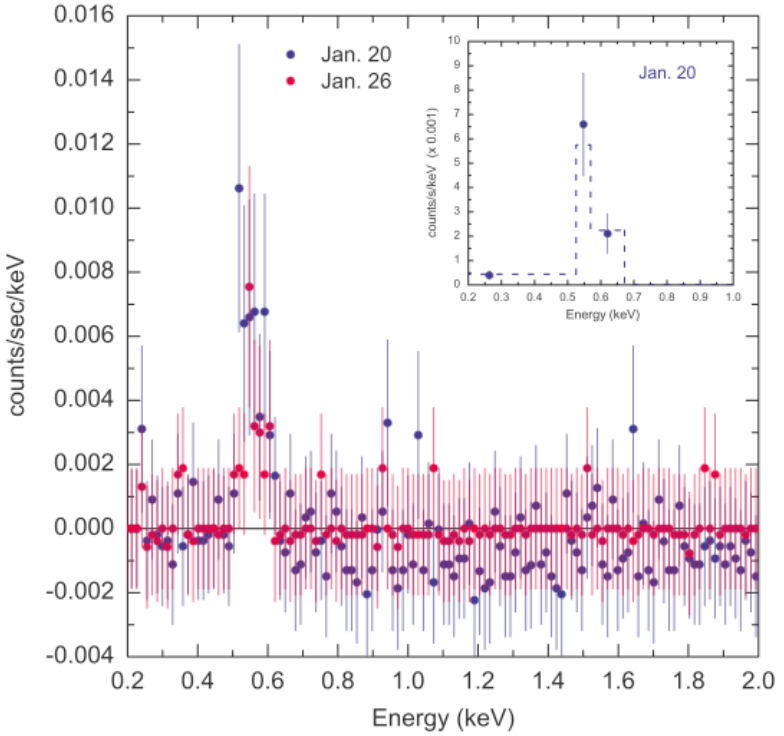

Fig. 42. Background-subtracted Chandra ACIS-S3-observed X-ray energy spectrum for Saturn's rings in the 0.2–2.0 keV range on 2004 January 20 and 26–27. The cluster of X-ray photons in the ∼0.49–0.62 keV band suggests the presence of the oxygen Kα line emission at 0.53 keV in the X-ray emission from the rings. The inset shows a Gaussian fit (peak energy = 0.55 keV, σ = 140 eV), shown by the dashed line, to the ACIS-observed rings' spectrum on January 20. Each spectral point (filled circle with error bar) represents ⩾10 measured events. The spectral fitting suggests that X-ray emissions from the rings are predominantly oxygen Kα

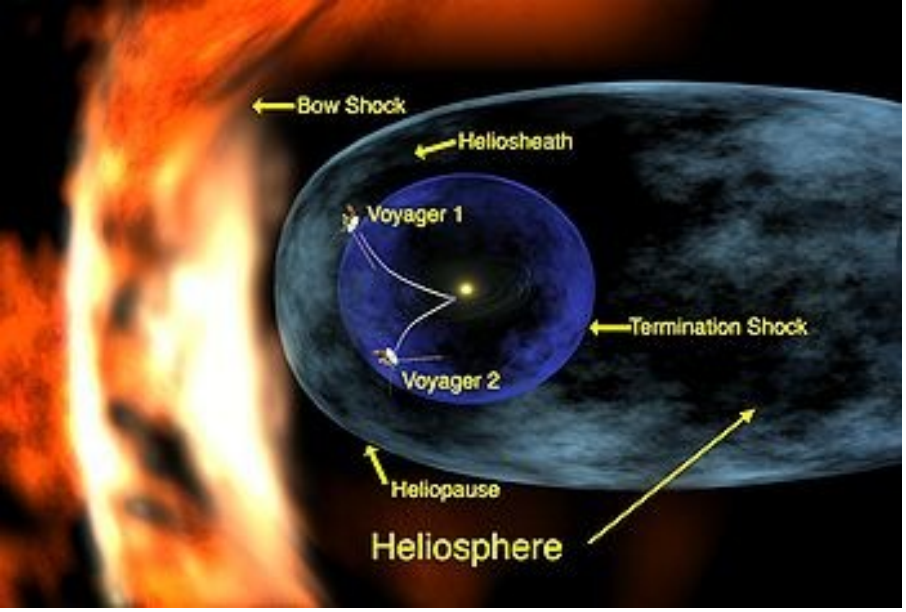

ROSAT LTEs

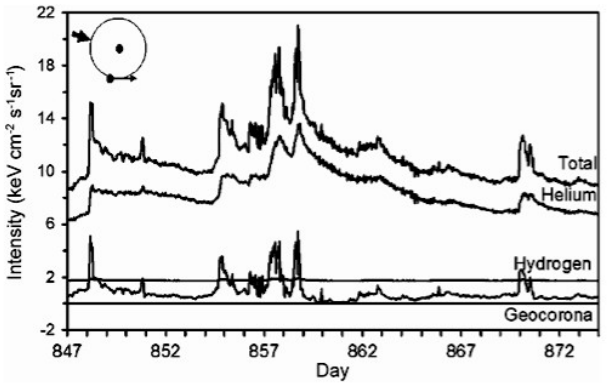

Fig. 44. SWCX X-ray intensities for a downwind direction. The direction of the interstellar wind is indicated with the thick arrow. The center of the circle is the Sun. The location of the Earth and the look direction are also indicated. The top curve is the total intensity and the labeled curves indicate the individual contributions to the total.

Cravens *et al*. 2002

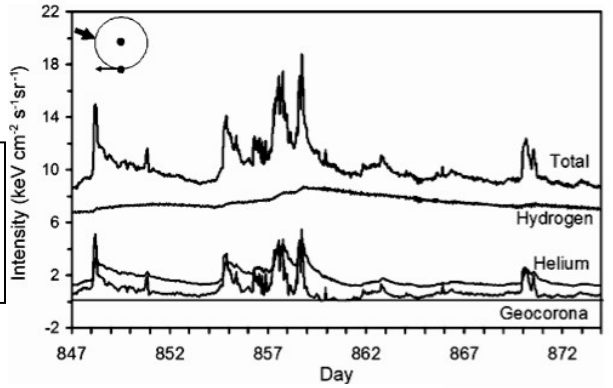

direction.

Instreaming neutral HI, HeI ISM gas create SWCXE X-rays in the Heliosphere

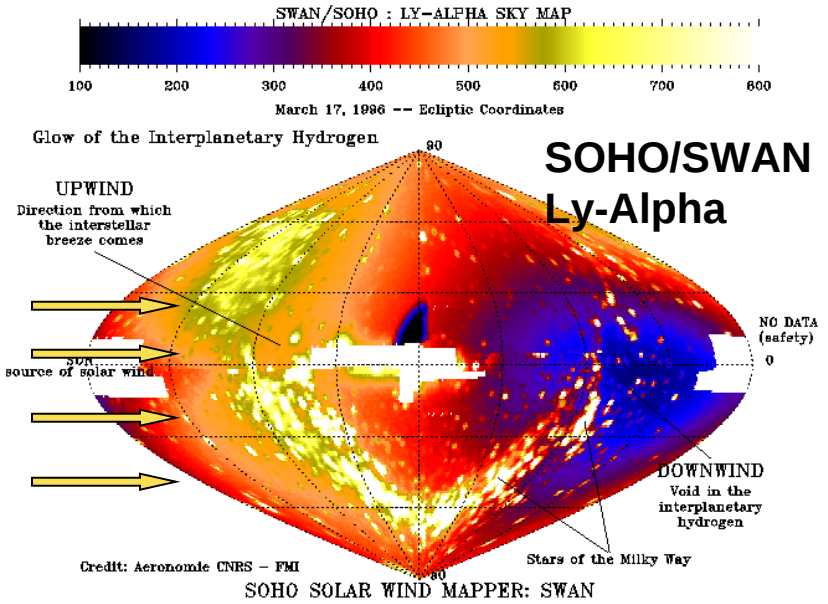

SOHO/SWAN Ly-Alpha

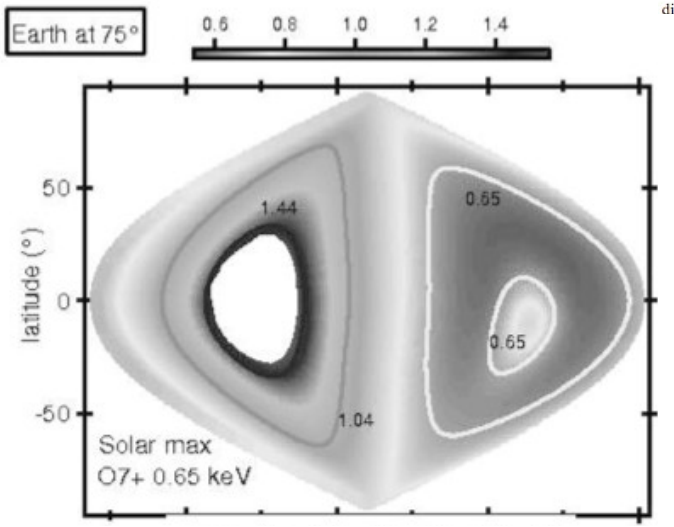

Koutroumpa *et al*. 2008

SWCXE spectral signature in heliospheric "background" observations.

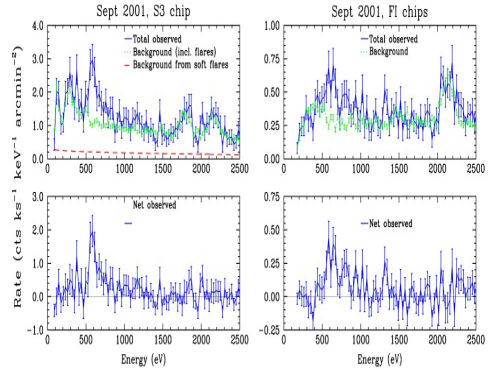

Fig. 14. Observed and background-subtracted spectra from the September 2001 Chandra observation of the dark side of the Moon, with 29-eV binning. Left panel is from the higher-QE but lower-resolution ACIS S3 CCD; right panel shows the higher-resolution ACIS front-illuminated (FI) CCDs. Oxygen emission from charge exchange is clearly seen in both spectra, and energy resolution in the FI chips is sufficient that O Lyman α is largely resolved from O Kα. High-n H-like O Lyman lines are also apparent in the FI spectrum, along with what is likely Mg Kα around 1340 eV. From Wargelin et al. (2004).

ACIS-S Lunar night-side emission, Wargelin *et al. 2004* (see also Wargelin *et al.* 2009 Chandra posters @ this meeting)

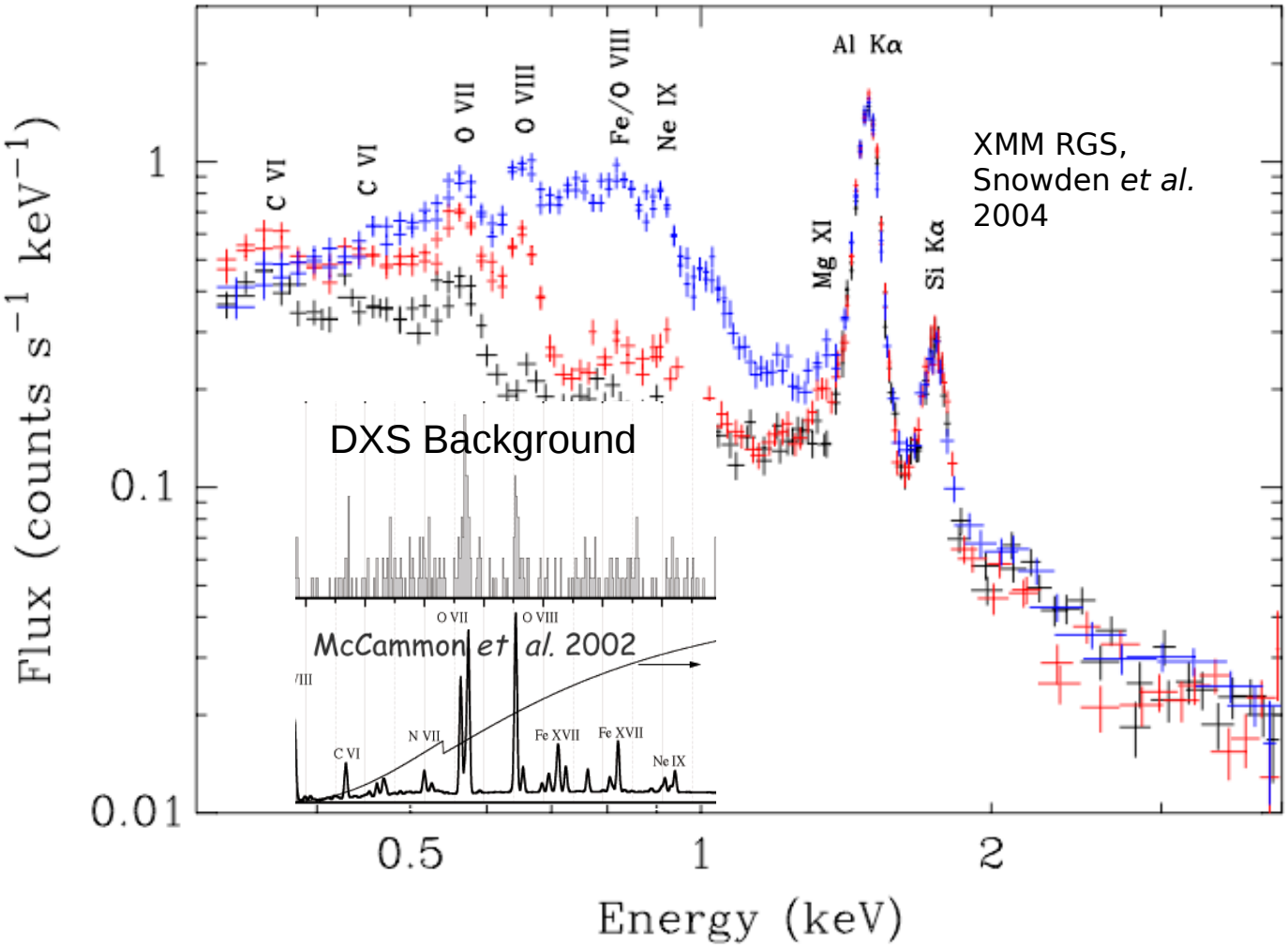

Fig. 49. XMM-Newton MOS spectra from two directions on the sky are plotted. The blue spectrum is from a relatively bright region near the Galactic center (l,b~348.6,22.4) while the red and black spectra are from a relatively dim region at higher latitude (l,b~125.9,54.8). The excess of the red spectrum over the black is from SWCX. The Al Kalpha and Si Kalpha lines are instrumental but the other lines are astrophysical in origin.

The Study of Solar System X-rays is a Very Rich Field, Still Developing. Low Lx but important processes. Next Up : Mercury, Uranus? High Latitude & Main Belt Comets? Trojan Asteroids? Active Centaurs? YSO dust evolution? Other Astrospheres & the Soft (1/4 keV) X-ray Background?

Summary of the characteristics of soft X-ray emission from solar system bodies

Bhardwaj, Lisse, et al. 2007 & Encyclopedia of the Solar System II, 200

Object	Emitting region	Power emitted[a]	Special characteristics	Production mechanism
Earth	Auroral atmosphere	10–30 MW	Correlated with magnetic storm and substorm activity	Bremsstrahlung from precipitating electrons, and characteristic line X-rays from atmospheric neutrals due to precipitating electron impact, + (see note[b])
Earth	Non-auroral atmosphere	40 MW	Correlated with solar X-ray flux	Scattering of solar X-rays by atmosphere
Moon	Dayside	0.07 MW	Correlated with solar X-ray flux	Scattering and fluorescence due to solar X-rays by the surface elements on dayside.
	Geocoronal (Nightside)		Nightside emissions are ~1% of the dayside emissions	SWCX with geocorona
Venus	Sunlit atmosphere	50 MW	Emissions from ~120–140 km above the surface	Fluorescent scattering of solar X-rays by C and O atoms in the atmosphere
Mars	Sunlit atmosphere	1–4 MW	Emissions from ~110–130 km above the surface	Fluorescent scattering of solar X-rays by C and O atoms in the upper atmosphere
	Exosphere	1–10 MW	Emissions extend out to ~8 Mars radii	SWCX with Martian corona
Jupiter	Auroral atmosphere	0.4–1 GW	Pulsating (~20–60 min) X-ray hot spot in north polar region	Energetic ion precipitation from magnetosphere and/or solar wind + electron bremsstrahlung
Jupiter	Non-auroral atmosphere	0.5–2 GW	Relatively uniform over disk	Scattering of solar X-rays + possible ion precipitation from radiation belts
Saturn	Sunlit disk	0.1–0.4 GW	Correlated with solar X-ray flux	scattering of solar X-rays + Electron bremsstrahlung ?
Comets	Sunward-side coma	0.2–1 GW	Intensity peaks in sunward direction $\sim 10^5$–10^6 km ahead of cometary nucleus	SWCX with cometary neutrals
Io Plasma Torus	Plasma torus	0.1 GW	Dawn-dusk asymmetry observed	Electron bremsstrahlung + ?
Io	Surface	2 MW	Emissions from upper few microns of the surface	Energetic Jovian magnetospheric ions impact on the surface
Europa	Surface	1.5 MW	Emissions from upper few microns of the surface	Energetic Jovian magnetospheric ions impact on the surface
Rings of Saturn	Surface	80 MW	Emissions confined to a narrow energy band around at 0.53 keV.	Fluorescent X-ray emission from atomic oxygen in H_2O ice excited by incident solar X-rays + ?
Asteroid	Sunlit surface		Correlated with solar X-ray flux	Fluorescent X-ray emission from elements in the surface excited by incident solar X-rays
Heliosphere	Entire heliosphere	10^{16} W	Emissions vary with solar wind variation	SWCX with heliospheric neutrals

[a]The values quoted are those at the time of observation. X-rays from all bodies are expected to vary with time. For comparison the total X-ray luminosity from the Sun is 10^{20} W. SWCX = solar wind charge exchange = charge exchange of heavy highly ionized solar wind ions with neutrals.

[b]X-rays can also result from accelerated electrons over thunderstorm regions, i.e., related to the atmospheric electric circuit. However, there is no clear detection of such soft X-rays so far.

Table 2
Summary of the characteristics of soft X-ray emission from solar system bodies

Object	Emitting region	Power emitted[a]	Special characteristics	Production mechanism
Earth	Auroral atmosphere	10–30 MW	Correlated with magnetic storm and substorm activity	Bremsstrahlung from precipitating electrons, and characteristic line X-rays from atmospheric neutrals due to precipitating electron impact, + (see note[b])
Earth	Non-auroral atmosphere	40 MW	Correlated with solar X-ray flux	Scattering of solar X-rays by atmosphere
Moon	Dayside	0.07 MW	Correlated with solar X-ray flux	Scattering and fluorescence due to solar X-rays by the surface elements on dayside.
	Geocoronal (Nightside)		Nightside emissions are ~1% of the dayside emissions	SWCX with geocorona
Venus	Sunlit atmosphere	50 MW	Emissions from ~120–140 km above the surface	Fluorescent scattering of solar X-rays by C and O atoms in the atmosphere
Mars	Sunlit atmosphere	1–4 MW	Emissions from ~110–130 km above the surface	Fluorescent scattering of solar X-rays by C and O atoms in the upper atmosphere
	Exosphere	1–10 MW	Emissions extend out to ~8 Mars radii	SWCX with Martian corona
Jupiter	Auroral atmosphere	0.4–1 GW	Pulsating (~20–60 min) X-ray hot spot in north polar region	Energetic ion precipitation from magnetosphere and/or solar wind + electron bremsstrahlung
Jupiter	Non-auroral atmosphere	0.5–2 GW	Relatively uniform over disk	Scattering of solar X-rays + possible ion precipitation from radiation belts
Saturn	Sunlit disk	0.1–0.4 GW	Correlated with solar X-ray flux	scattering of solar X-rays + Electron bremsstrahlung ?
Comets	Sunward-side coma	0.2–1 GW	Intensity peaks in sunward direction $\sim 10^5$–10^6 km ahead of cometary nucleus	SWCX with cometary neutrals
Io Plasma Torus	Plasma torus	0.1 GW	Dawn-dusk asymmetry observed	Electron bremsstrahlung + ?
Io	Surface	2 MW	Emissions from upper few microns of the surface	Energetic Jovian magnetospheric ions impact on the surface
Europa	Surface	1.5 MW	Emissions from upper few microns of the surface	Energetic Jovian magnetospheric ions impact on the surface
Rings of Saturn	Surface	80 MW	Emissions confined to a narrow energy band around at 0.53 keV.	Fluorescent X-ray emission from atomic oxygen in H_2O ice excited by incident solar X-rays + ?
Asteroid	Sunlit surface		Correlated with solar X-ray flux	Fluorescent X-ray emission from elements in the surface excited by incident solar X-rays
Heliosphere	Entire heliosphere	10^{16} W	Emissions vary with solar wind variation	SWCX with heliospheric neutrals

[a]The values quoted are those at the time of observation. X-rays from all bodies are expected to vary with time. For comparison the total X-ray luminosity from the Sun is 10^{20} W. SWCX = solar wind charge exchange = charge exchange of heavy highly ionized solar wind ions with neutrals.

[b]X-rays can also result from accelerated electrons over thunderstorm regions, i.e., related to the atmospheric electric circuit. However, there is no clear detection of such soft X-rays so far.

Spectral Modeling & Lab Measurements of Cometary CXE

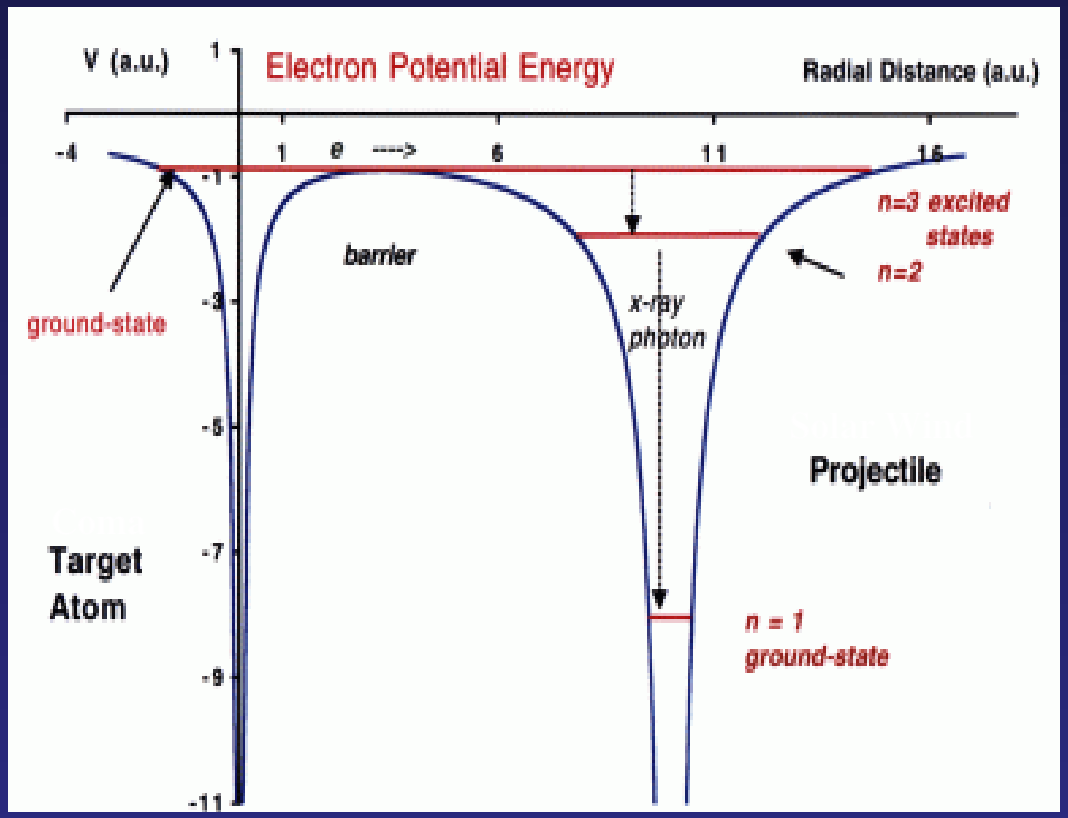

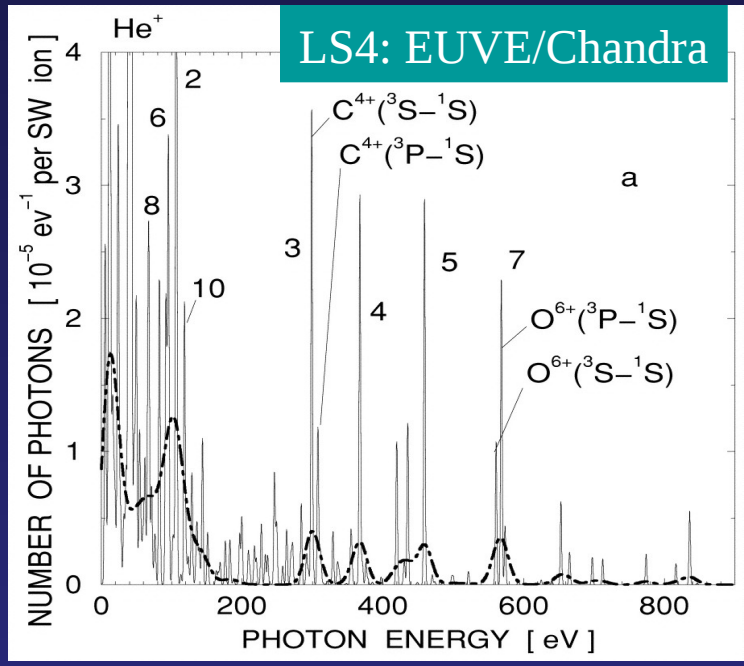

- OVII/OVII line ratios variable
- He^+,background signal huge at E < 250 eV
- All lines, or lines + continuum?
- Fast vs slow solar wind - expect different spectra
- Auger e^- quenching on dust, surfaces (Hale-Bopp)?
- Role of Collisions in the cometary atmosphere?

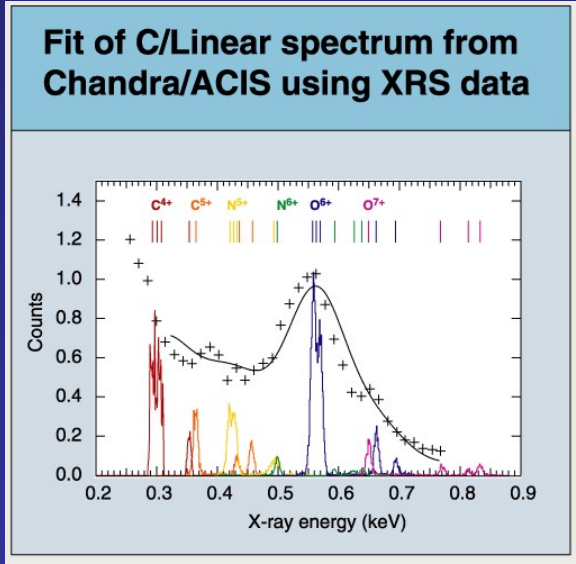

Solar Wind Elements/Isotopes Observed by

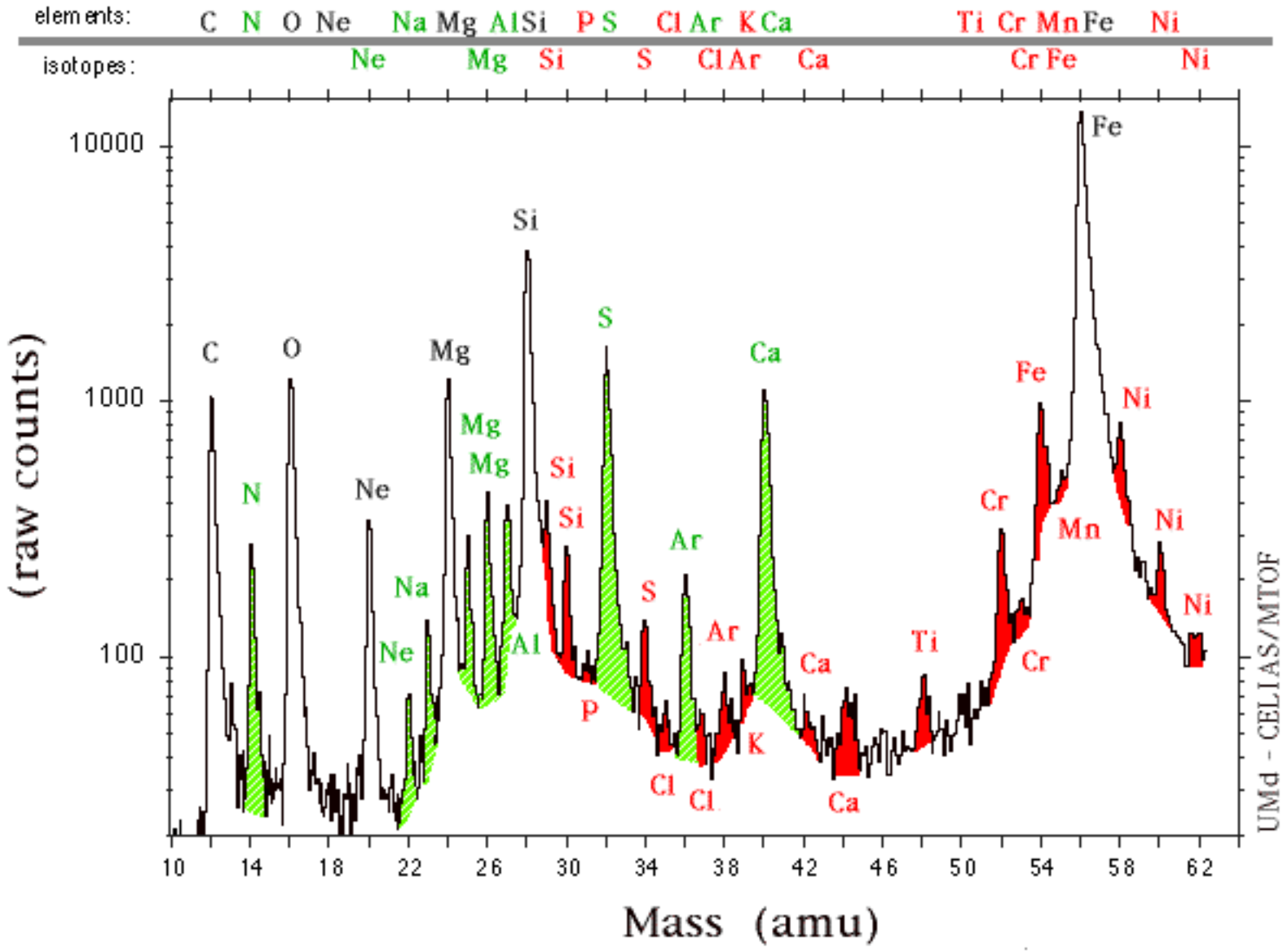

X-ray lightcurve of 9P/Tempel 1

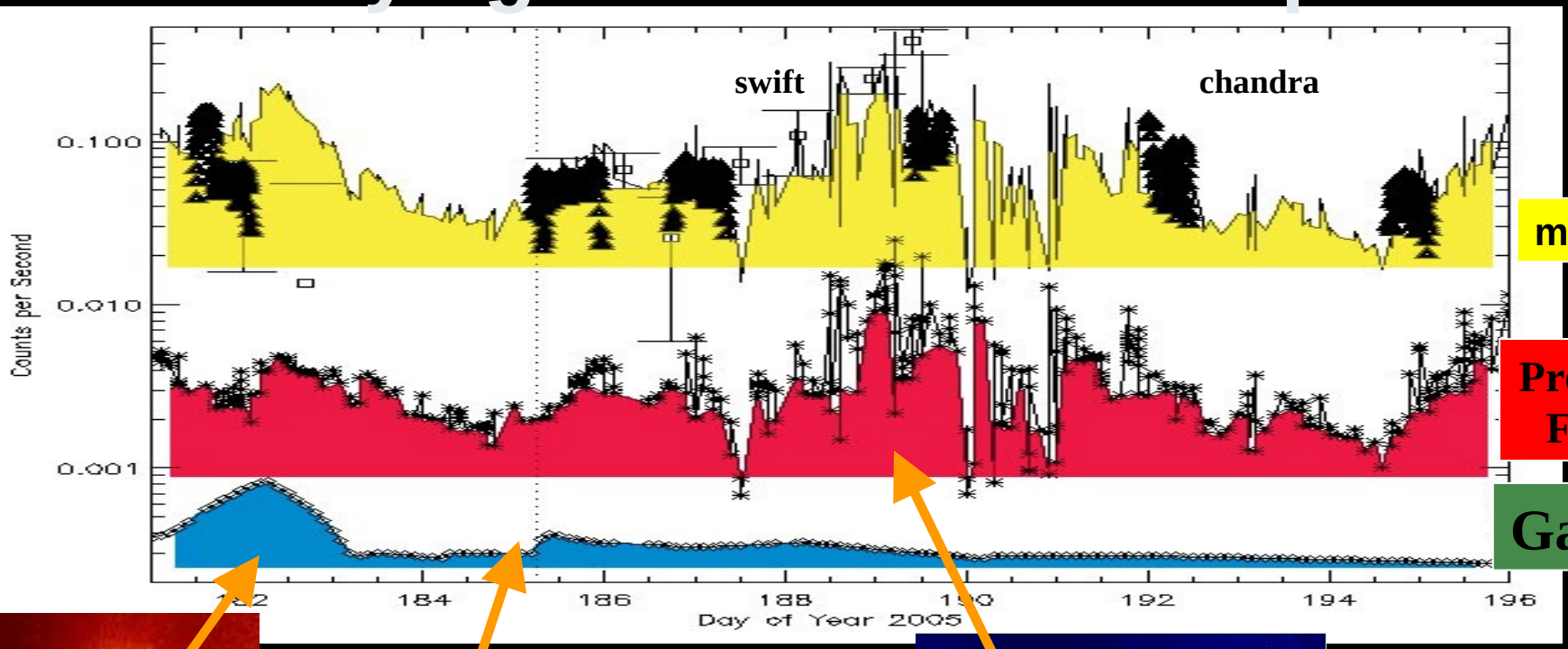

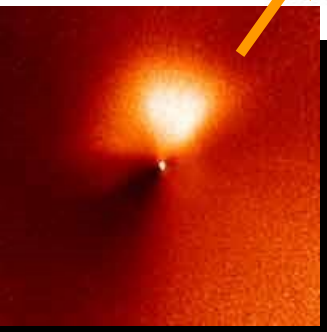

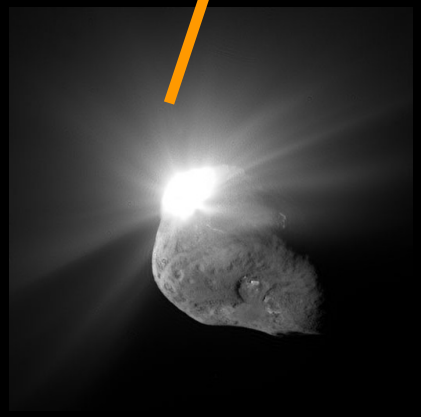

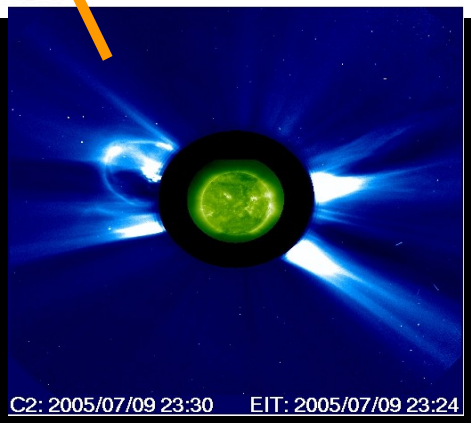

Swift data from Willingale et al ('06)
Gas production from Schleicher ('06) and Lisse ('06)

- No prompt X-ray flash
- Increase X-ray flux < 20% → consistent with coma observations (Kuppers '05, Keller '05, Farnham '07)

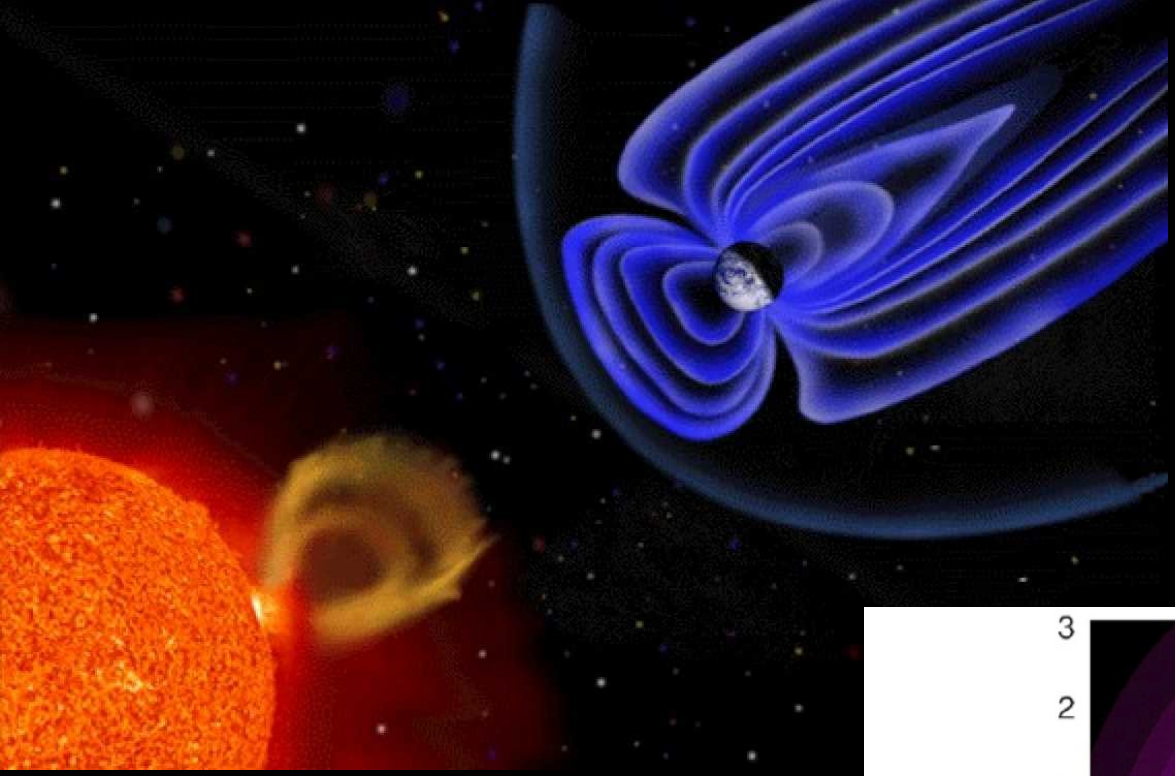

SWCX Processes in the Earth's GeoCorona.

Detection of heavy neutral atoms in the Earth's magnetosphere implies interaction of the extended cold H envelope of the Earth with the solar wind via CXE

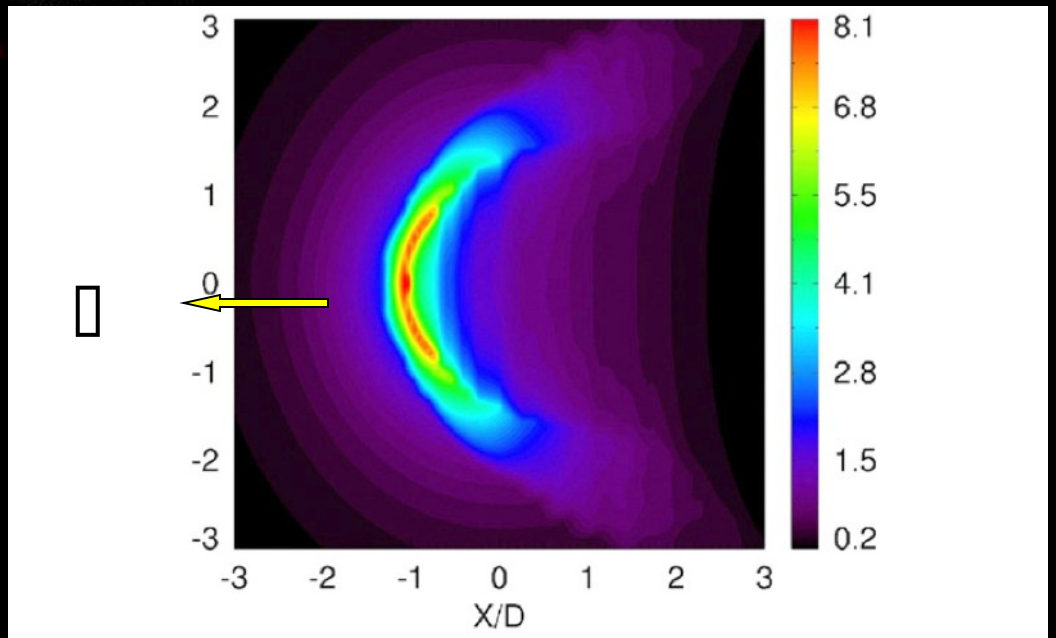

Fig. 12. Image of the X-ray intensity as observed from the Earth's flanks in the equatorial plane. Brightness scale units are keV/cm^2/s/sr. *R* and *X* are coordinates in the image plane. Units are in D (distance to the magnetopause). From Robertson and Cravens (2003a, b).

N.B. - SWCX more important than Jeans escape for terrestrial H loss budget.

Evidence : - Atmosphere Explorer C 1974

- Arecibo Incoherent Scatter Radar of e- and neutral H abundances (Maher and Tinsley 1977)
- IMAGE/LENA observations of magnetosheath quiescent solar behavior (Collier *et al*. 2001)
- IMAGE/HENA - CME response (Brandt 2001)

Simulated X-ray images using detailed atmospheric and exospheric models of Venus for ..

.. scattering of solar X-rays

(logarithmic intensity scale)

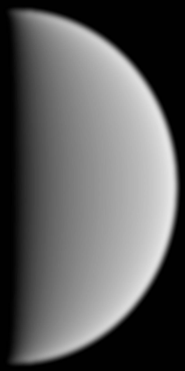

~ solar maximum

Dennerl et al. 2002, A&A 386

.. solar wind charge exchange

(logarithmic intensity scale)

Gunell et al. 2007, GRL 34

Simulated X-ray images using detailed atmospheric and exospheric models of Venus for ..

.. scattering of solar X-rays

(logarithmic intensity scale)

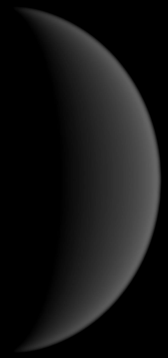

~ solar minimum

Dennerl et al. 2002, A&A 386

.. solar wind charge exchange

(logarithmic intensity scale)

Gunell et al. 2007, GRL 34

Charge exchange at Mars

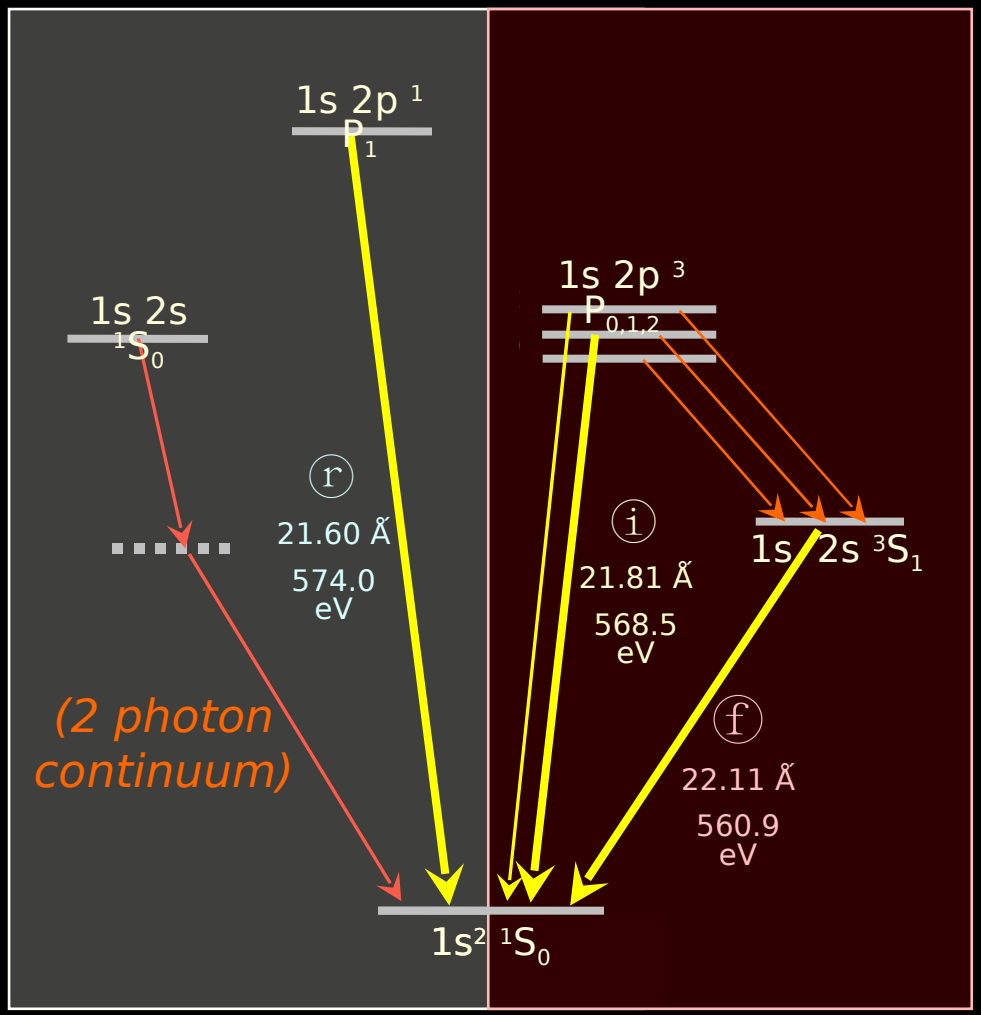

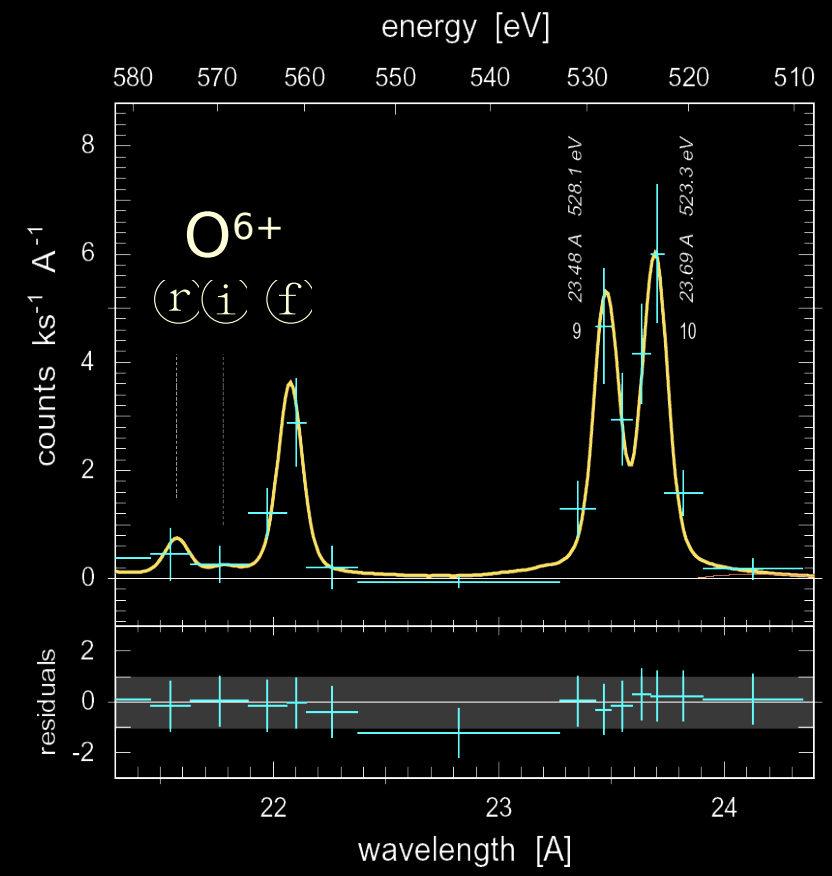

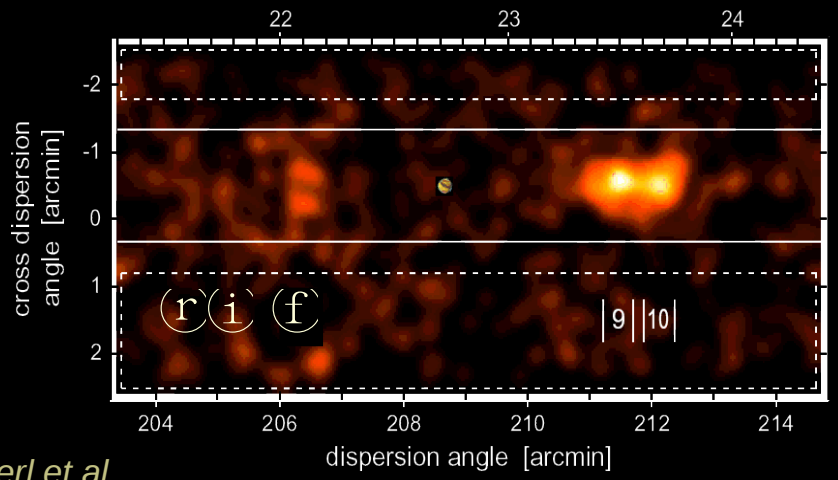

Dennerl et al. 2006

X-ray Emission from the North Pole

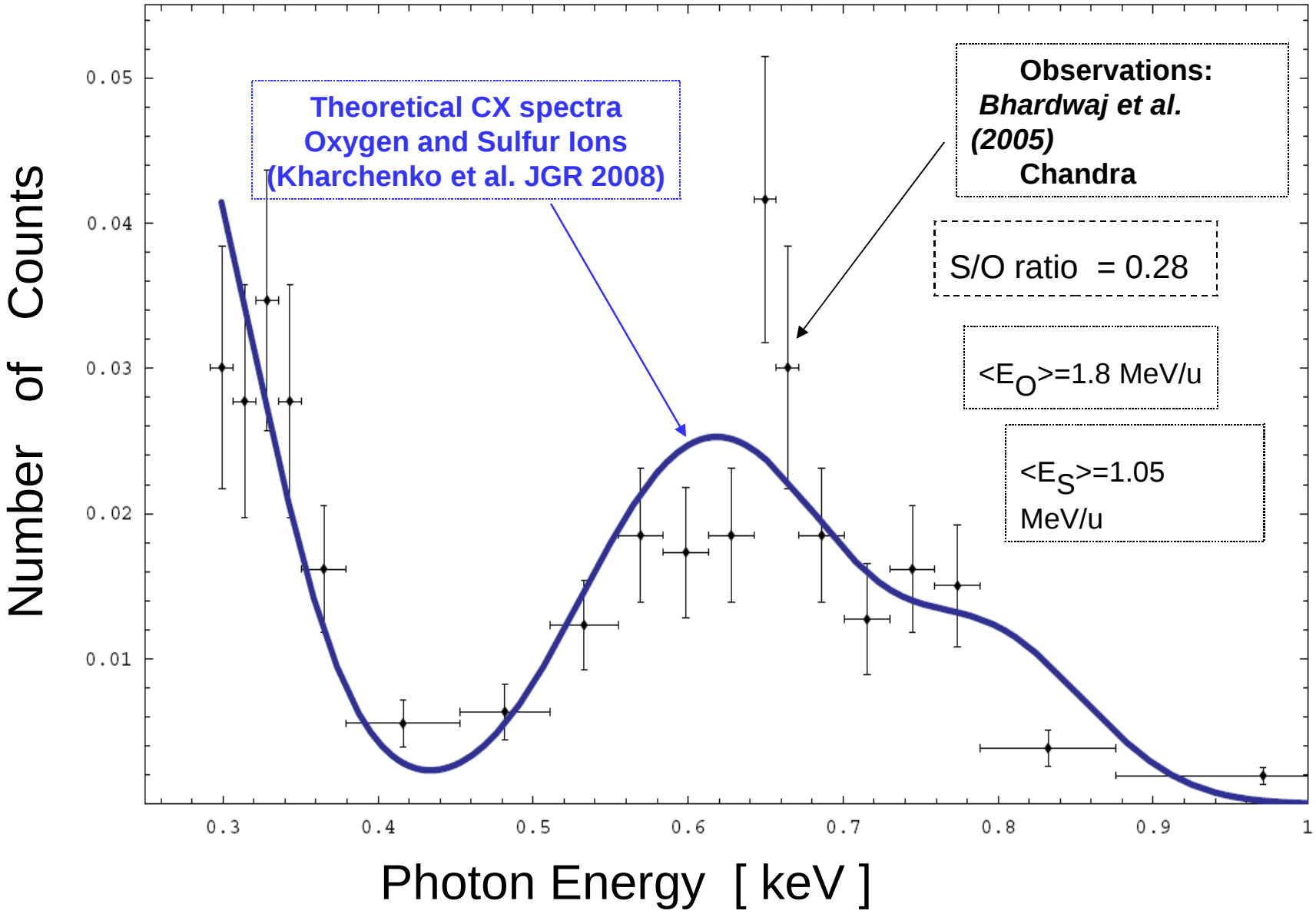

~40-min Periodicity Seen in X-rays and THz Radio, But Not by Galileo and Cassini s/c in Any Other Passband!

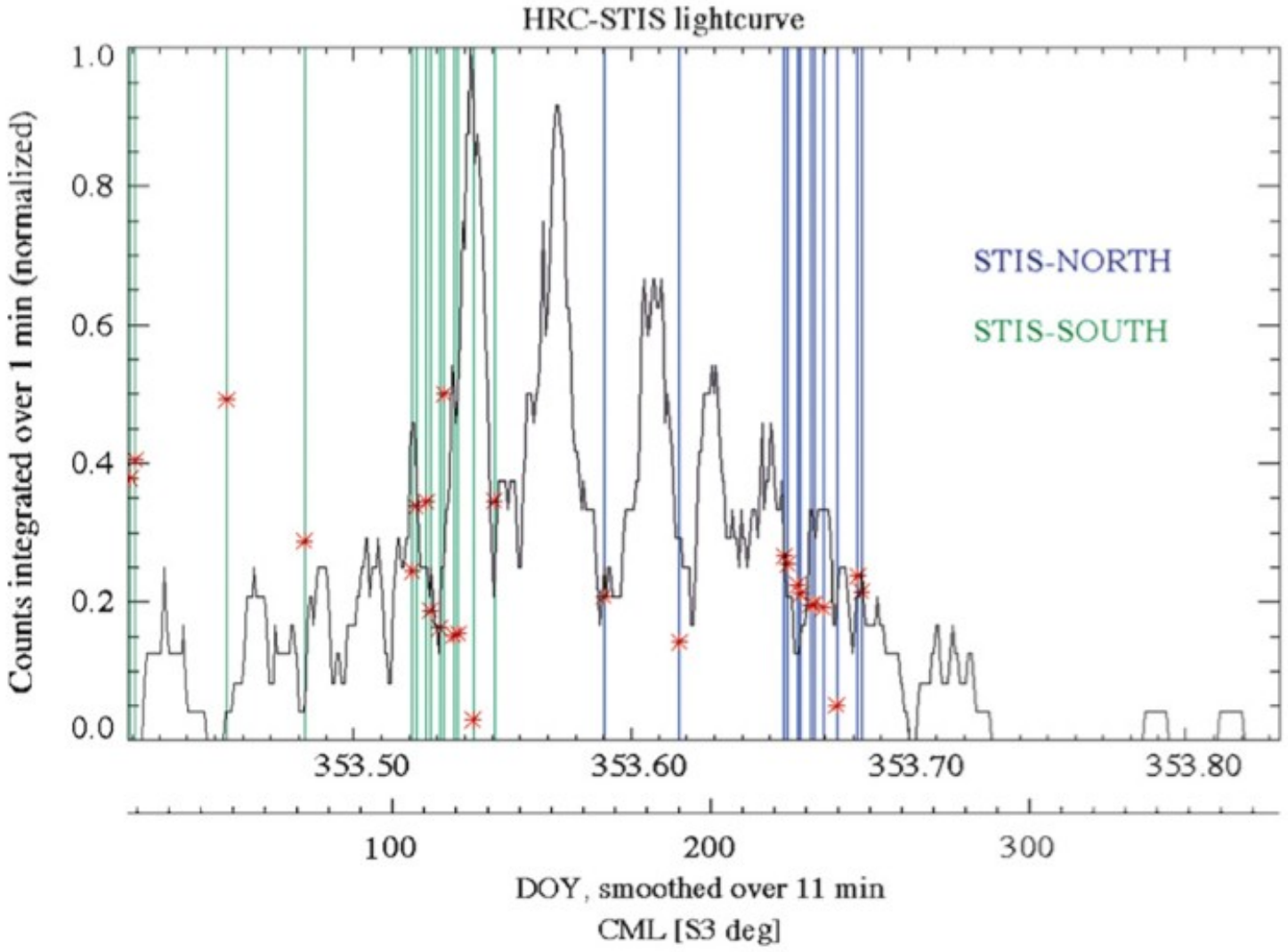

Fig. 23. X-ray intensity variation with time indicating the 40 m periodicity at high northern latitudes of Jupiter.

Studies of Planets and Comets in the X-ray

C.M. Lisse *(JHU Applied Physics Laboratory*)**; A. Bhardwaj** *(SPL, Vikram Sarabhai Space Centre*)**; K. Dennerl** *(MPI für extraterrestrische Physik)*; **S. J. Wolk** *(Chandra X-ray Center)***D. J. Christian** *(Queens University Belfast)*;; **D. Bodewits** *(NASA/GSFC)*; **T.H. Zurbuchen** *(University of Michigan)*

Chandra's First Decade of Discovery

Boston, MA, 25 Sept 2009

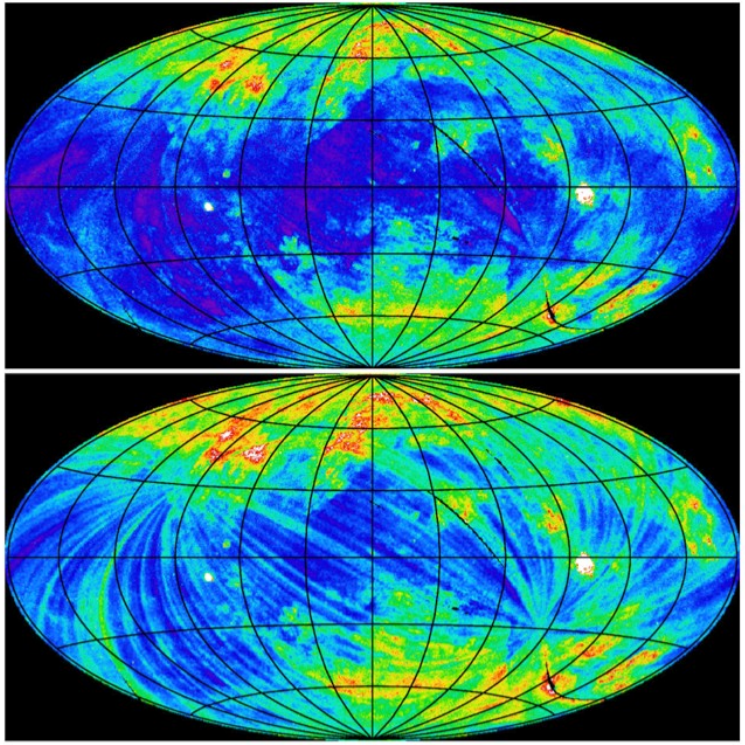

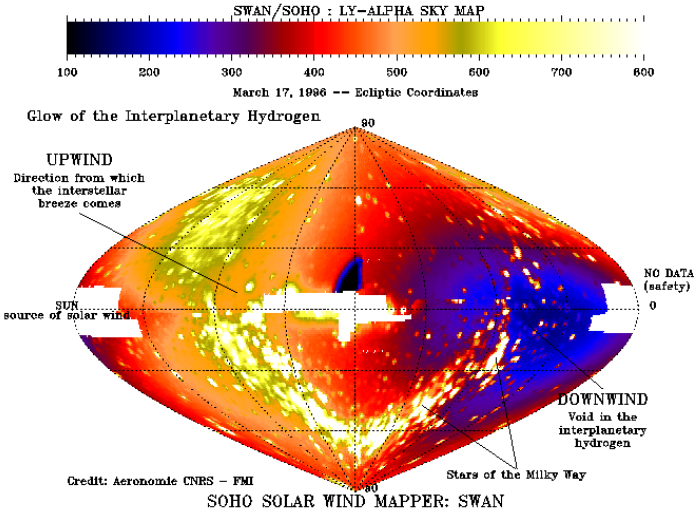

Fig. 47. Upper panel: ROSAT All-Sky Survey map of the cosmic X-ray background at $\frac{1}{4}$keV (Snowden et al., 1997). The data are displayed using Aitoff projection in Galactic coordinates centered on the Galactic center with longitude increasing to the left and latitude increasing upwards. I intensity is indicated by purple and blue while red indicates higher intensity. Lower panel: Same as above except the contaminating LTEs (SW emission) were not removed. The striping is due to the survey geometry where great circles on the sky including the ecliptic poles were scanned precess at ~1°/day.

Shape of Soft SWCXE Heliospheric Emission Follows One-Half the Ecliptic Sphere on the Sky (Planar ISM Source)

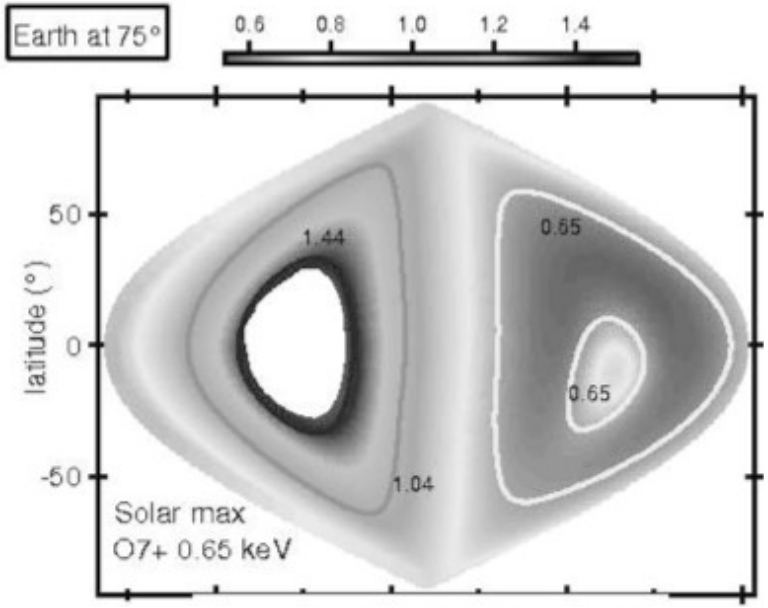

Koutroumpa *et al*. 2008